

13. A PALEONTOLOGICAL SYNTHESIS OF ODP LEG 210, NEWFOUNDLAND BASIN¹

E. Urquhart,² S. Gardin,³ R.M. Leckie,⁴ S.A. Wood,⁵ J. Pross,⁶
M.D. Georgescu,⁷ B. Ladner,⁸ and H. Takata⁹

ABSTRACT

Sediments recovered from Ocean Drilling Program Leg 210 Hole 1276A range in age from Early Cretaceous (earliest Albian) to Paleogene (earliest Oligocene). In this study, samples were processed and analyzed for micropaleontological and palynological content, as well as sedimentary components. Core recovery from this site was good (85% between 800 and 1725.16 meters below seafloor), and the majority of samples processed yielded microfossils of some nature. Although none of the major groups are consistently present in all samples, calcareous nannofossils, agglutinated benthic foraminifers, and radiolarians do occur in many samples. The best age constraints for Hole 1276A are provided by calcareous nannofossils and dinoflagellate cysts. Age-diagnostic planktonic foraminifers are more commonly found in redeposited turbidite sandstones rather than in the autochthonous pelagic mudrocks. The depositional environments of the sediments have been interpreted as varying in oxygenation but having been deposited at abyssal depths (>2000 m) near or below the calcite carbonate depth (CCD). Almost uninterrupted deepwater deposition since the Aptian is evidenced both by the evolutionary succession of biota recovered from the sediments and by the sedimentary history of turbidites and gravity flow deposits derived from neritic and bathyal sources on the adjacent margin. A condensed interval recorded in the Turonian–Maastrichtian is likely associated with sediment starvation at times of high global sea level. A disconformity and condensed interval in the lower middle Eocene (~48.5–43.7 Ma) is associated with a change in global sea level and may be associated with invigorated deepwater current activity. Anoxic conditions affected the deep seafloor of the North Atlantic during Oceanic Anoxic Event

¹Urquhart, E., Gardin, S., Leckie, R.M., Wood, S.A., Pross, J., Georgescu, M.D., Ladner, B., and Takata, H., 2007. A paleontological synthesis of ODP Leg 210, Newfoundland Basin. *In* Tucholke, B.E., Sibuet, J.-C., and Klaus, A. (Eds.), *Proc. ODP, Sci. Results*, 210: College Station, TX (Ocean Drilling Program), 1–53. doi:10.2973/odp.proc.sr.210.115.2007

²RSMAS, University of Miami, 4600 Rickenbacker Causeway, Miami FL 33149, USA.

eurquhart@rsmas.miami.edu

³CNRS UMR 5341, Université Pierre et Marie Curie, 4 Place Jussieu, Case 104, Paris Cedex 05 75353, France.

⁴Department of Geosciences, University of Massachusetts, 611 North Pleasant Street, Amherst MA 01003, USA.

⁵12155 Lucille Lane, Anchorage AK 99515, USA.

⁶Institute of Geosciences, Johann Wolfgang Goethe University, Allee 1, Frankfurt D-60438, Germany.

⁷University of Saskatchewan, Department of Geological Sciences, 114 Science Place, Saskatoon SK S7N 5E2, Canada. Present address:

Geoscience, University of Calgary, 2500 University Drive NW, Calgary, Alberta T2N 1N4, Canada.

⁸Total Biostratigraphic Services, Inc., 7000 Ute Court, Ocean Springs MS 39564, USA.

⁹Research Center for Coastal Lagoon, Shimane University, 1060 Nishikawatsu, Matsue 690-8504, Japan.

Initial receipt: 2 March 2007

Acceptance: 10 July 2007

Web publication: 27 July 2007

Ms 210SR-115

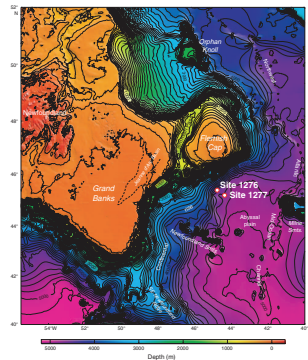
(OAE) 1b (earliest Albian, ~112 Ma) and OAE2 (Cenomanian–Turonian boundary interval, ~93.5 Ma). Cooling during the early Turonian followed the vast carbon burial associated with OAE2 based on calcareous nannofossil assemblages. The recovery of a nearly complete Cretaceous–Paleogene boundary transition represents one of the deepest-water records of the end-Cretaceous event known. Another important paleontological discovery from Hole 1276A was the redeposited large-size benthic foraminifers of Campanian–Maastrichtian and latest Paleocene–early Eocene ages, which point to a nearby source of shallow, warm-water carbonates during these two periods of global warmth.

INTRODUCTION

Ocean Drilling Program (ODP) Leg 210 Site 1276 is located in the deep Newfoundland Basin, east of the Grand Banks and south of the Flemish Cap (45°24.3198'N, 44°47.1496'W) in 4549 m of water (Tucholke, Sibuet, Klaus, et al., 2004). The site was cored in the interval from 800.0 to 1736.9 meters below seafloor (mbsf) with 85% core recovery. The principal scientific objectives of ODP Leg 210 focused on the rifting and postrift sedimentation of the Newfoundland continental margin in relation to the conjugate Iberian continental margin. They represent nonvolcanic rifted margins, and ODP Leg 210 is the first coring on the western side of the rift. Site 1276 was drilled on transitional crust adjacent to oceanic crust of probable Barremian age based on the interpretation of magnetic Anomaly M3 (Tucholke, Sibuet, Klaus, et al., 2004) (Fig. F1). Site 1277 was drilled on a shallow basement high ~40 km southeast of Site 1276. Secondary drilling objectives of ODP Leg 210 included the paleoceanographic history at the northern edge of the central North Atlantic as the gateway to the northern North Atlantic began to open during the Early Cretaceous. The Cretaceous–Paleogene interval was a time of major paleoceanographic events including oceanic anoxic events of the mid-Cretaceous, the Cretaceous/Paleogene boundary, and the Paleocene/Eocene Thermal Maximum. In addition, seafloor spreading and ocean gateway deepening and widening at both ends of the central North Atlantic played a major role in changing surface and deepwater circulation during this time.

From Hole 1276A we recovered a 936.9-m-thick succession of mudrock, shale, and interbedded turbidite sandstone and other gravity flow deposits spanning ~80 m.y. of the mid-Cretaceous to early Oligocene (~113–33 Ma). Despite the pervasive redeposited nature of the sedimentary succession cored at Site 1276, the paleontological findings reported here provide a robust temporal framework for the largely uninterrupted record of changing paleoenvironmental conditions of the surface ocean and in the deep Newfoundland Basin. This synthesis incorporates new paleontological results since the publication of the Leg 210 *Initial Reports* volume (Tucholke, Sibuet, Klaus, et al., 2004). It provides a detailed revision of the calcareous nannofossil biostratigraphy, as well as an updated discussion of sedimentation history and comprehensive summary of North Atlantic paleoceanography based on paleontological data from Site 1276. Site 1277 is not included in this analysis because of the paucity of sediment and lack of age-diagnostic fossils.

F1. Bathymetry of the Newfoundland margin, p. 36.



MATERIALS AND METHODS

Method of Study for Calcareous Nannofossils

Calcareous nannofossils were examined in strewn slides using standard light microscope techniques under cross-polarized and phase-contrast light at 625× magnification on a Zeiss Axiophot. Settled strewn slides were prepared by mixing a small amount of sediment with 1–2 mL of buffered, distilled water, which was then thoroughly mixed with a plastic pipette. The mixture was distributed on a 22 mm × 40 mm glass coverslip, which was then dried on a slide warmer until all of the water had evaporated. The dried coverslip was then adhered to the slide with three drops of Norland-61 optical adhesive, and the adhesive was cured under ultraviolet light.

The following abbreviations are used to describe nannofossil preservation:

- G = good preservation (little or no evidence of dissolution and/or recrystallization; primary morphological characteristics only slightly altered; specimens were identifiable to the species level).
- M = moderate preservation (specimens exhibit some etching and/or recrystallization; primary morphological characteristics somewhat altered; however, most specimens were identifiable to the species level).
- P = poor preservation (specimens were severely etched or overgrown; primary morphological characteristics largely destroyed; fragmentation has occurred; specimens often could not be identified at the species and/or generic level).

Five calcareous nannofossil abundance levels are recorded as follows:

- V = very abundant; 11–100 specimens/field of view (FOV).
- A = abundant; 1–10 specimens/FOV.
- C = common; 1 specimen/2–10 FOV.
- F = few; 1 specimen/11–100 FOV.
- R = rare; 1 specimen/101+ FOV.

The same definitions are used for estimations of total abundance of each sample, with the additional definition of “B” (B = barren of nannofossils). This abundance scheme allows comparison of Site 1276 results with those obtained on the conjugate Iberian margin at Deep Sea Drilling Project (DSDP) Site 398 and ODP Sites 1067 through 1069 (Blechschmidt, 1979; McGonigal and Wise, 2001).

The zonal scheme of Bukry (1973, 1975; zonal code numbers CN and CP added and modified by Okada and Bukry, 1980) is used for Cenozoic calcareous nannofossil biostratigraphy. The zonal schemes of Sissingh (1977; CC zones), as modified by Perch-Nielsen (1985), Applegate and Bergen (1988; Lower Cretaceous subzones), and Burnett (1998; UC zones) are used for the Late Cretaceous, and those of Roth (1973, 1983; NC zones), with subdivisions by Bralower et al. (1993), are used for the Early Cretaceous. Age estimates for calcareous nannofossil first and last occurrences are summarized in Tucholke, Sibuet, Klaus, et al. (2004).

Method of Study for Microfossils Larger Than 63 μm

Unlithified sediments were soaked in a 3% solution of hydrogen peroxide (H_2O_2), warmed on a hot plate ($\sim 50^\circ\text{C}$) for 20 min, and then washed with tap water over a 63- μm sieve. Samples within 0.5 m above the Cretaceous/Tertiary boundary were washed over a 38- μm sieve to catch the dwarf microfossil assemblages, and samples from the Lower Cretaceous interval were washed over a 45- μm sieve. Lithified sediments were first mechanically crushed into <1 cm fragments and then treated in the same manner. All samples (residues >63, 45, or 38 μm) were dried on filter paper on a hotplate at $\sim 50^\circ\text{C}$ and then sieved through a sieve tower of 125-, 250-, and 500- μm meshes. Samples were examined for age-diagnostic species of planktonic foraminifers on the >250- μm , 125- to 250- μm , and 63- to 125- μm size fractions. In addition, all size fractions were carefully scanned for other biotic (e.g., radiolarians, sponge spicules, echinoid spines, fish bone/teeth, ostracodes, and inoceramid prisms) and mineral (glauconite, pyrite, and phosphate pellets) constituents of the sand-sized residues.

The following abundance categories used in the text were estimated from visual examination of the dried sample for biotic constituents and for mineral grains >63 μm :

- D = dominant (>30%).
- A = abundant (10%–30%).
- F = few (5%–10%).
- R = rare (1%–5%).
- P = present (<1%).

The preservation status of the recovered microfossils >63 μm is estimated as follows:

- VG = very good; no evidence of overgrowth, dissolution, or abrasion.
- G = good; little evidence of overgrowth, dissolution, or abrasion.
- M = moderate; calcite overgrowth, dissolution, or abrasion are common, but minor.
- P = poor; substantial overgrowth, dissolution, or fragmentation.

The tropical Paleogene planktonic foraminiferal zonal scheme (P zones) follows Berggren et al. (1995). The zonation used for Cretaceous planktonic foraminifers is based on the tropical zonal schemes of Caron (1985) and Sliter (1989; KS zones), with modifications by Bralower et al. (1993, 1995a, 1997) and Premoli Silva and Sliter (1994, 1999). Age estimates for planktonic foraminifer first and last occurrences are summarized in Tucholke, Sibuet, Klaus, et al. (2004).

PALEONTOLOGICAL RESULTS

The sedimentary succession cored at Site 1276 was deposited at abyssal depths (>2000 m) near or below the calcite compensation depth (CCD) throughout its post-Aptian history based on the general paucity of carbonate microfossils, particularly the planktonic foraminifers, and the dominance of deepwater agglutinated benthic foraminifers and variable quantities of radiolarians, phosphatic fish debris, sponge spicules, and plant debris in the in situ mudrock and shale (Tucholke,

Sibuet, Klaus, et al., 2004). Calcareous nannofossils fared much better than the planktonic foraminifers against the ravages of dissolution, probably owing to their transport to the seafloor in zooplankton fecal pellets or marine snow (Honjo, 1975, 1976; Pilskaln and Honjo, 1987; Steinmetz, 1994). Although the calcareous nannofossils show variable abundance and preservation through the section, they provide excellent biostratigraphic control in most sampled intervals.

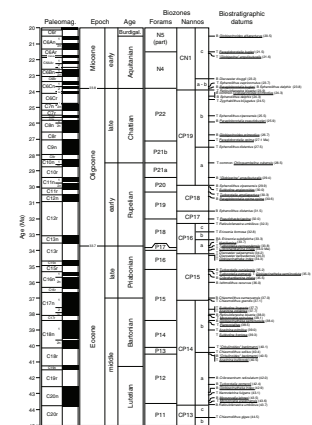
Most of the in situ mud rock samples investigated are barren of planktonic foraminifers. A relatively few number of samples contain rare to few specimens (<50 tests), and fewer still contain age-diagnostic planktonic foraminiferal assemblages. However, thin sections of Cretaceous and Paleogene sandstones yield redeposited age-diagnostic planktonic foraminifers. Between the pelagic and allochthonous sediments, a planktonic foraminiferal biostratigraphy has emerged that is complementary to that of the calcareous nannofossils. The calcareous nannofossil and planktonic foraminifer zonal schemes utilized in this study are shown in Figure F2. Zonal marker species (i.e., those species whose first and last occurrence datums are used to delimit the boundaries of the zones) are shown along the right, together with other useful secondary marker species. However, the pervasive presence of reworked taxa prevents reliable recognition of important last occurrences that characterize some biozones in time intervals such as the Cenomanian–Turonian, Campanian, Maastrichtian, Paleocene–Eocene, and Eocene–Oligocene transitions.

Most foraminiferal samples (>38- or >63- μm residues) contain fairly diverse and generally well preserved assemblages of in situ abyssal agglutinated benthic foraminifers (e.g., Kuhnt and Urquhart, 2001; Takata, 2007). Some of these samples also contain siliceous microfossils such as radiolarians and diatoms, as well as phosphatic fish teeth or bone fragments. Palynomorphs (predominantly dinocysts and sporomorphs) are very well preserved in organic-rich, dark-colored sediments, and although spot sampled, they provide a critical component of the biostratigraphic age control for the site. In the oldest part of the cored section, common carbonized plant debris is a characteristic component in washed residues. A summary of the microfossil biostratigraphy is compared to lithology and core recovery in Figure F3.

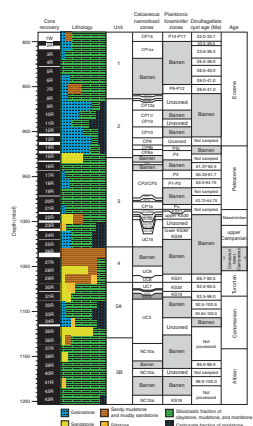
Where present, planktonic and calcareous benthic foraminifers are often very small (<125 μm). They likely are size-sorted by processes associated with downslope transport in turbidity currents, a supposition that is based on the size of the co-occurring quartz grains. Calcareous benthic foraminifers indicate that the source areas for the turbidites cored at Site 1276 have varied through the section from neritic (<200 m) to bathyal (200–2000 m) depths along the adjacent continental margin. Reworking of Upper Cretaceous material is prevalent in the Paleogene, but redeposition processes were largely penecontemporaneous during the Cretaceous, based on a uniform age progression of the samples and minimal reworking of older material in calcareous nannofossil, palynomorph, and foraminifer samples (Tucholke, Sibuet, Klaus, et al., 2004).

The presence, preservation, diversity, associations, and abundance of the microfossil assemblages, together with mineral residues, have been used to interpret the probable changing depositional environments of the site during the history of this evolving ocean–continent transition. The descriptive sections are followed by an interpretation section that addresses depositional processes, paleoceanography, and sediment provenance and diagenesis as appropriate. In many cases, the interpre-

F2. Calcareous nannofossil and planktonic foraminiferal zonal schemes, p. 37.



F3. Microfossil biostratigraphy, p. 41.



tations are provisional, bearing in mind the difficulty of interpreting a sedimentary basin using only a single linear stratigraphic section.

The cored section of Hole 1276A was divided into lithostratigraphic units (Unit 5, the oldest, through Unit 1, the youngest) (Tucholke, Sibuet, Klaus, et al., 2004), and the biotic components are discussed below in relation to these host sediments. Much of the material penetrated at Site 1276 has been classed as turbidites, gravity flow deposits, and pelagic muds (grainstone, sandstone, sandy mudstone, and mudstone, with marlstone in Unit 2 and black shale and claystone in Unit 5). Although turbidites have generally been considered unreliable for biostratigraphy, those turbiditic deposits analyzed as part of this study together with the in situ pelagic background sediments are considered to contain contemporaneous fossils, unless otherwise noted. Descriptions of the host sediments are brief summaries which include notes directly relevant to the micropaleontological and palynological biostratigraphic and paleoenvironmental interpretations. Comprehensive lithologic descriptions can be found in the Leg 210 *Initial Reports* volume (Tucholke, Sibuet, Klaus, et al., 2004).

BIOSTRATIGRAPHY OF SITE 1276

Lithologic Subunit 5C

Age: (latest Aptian?) early to middle Albian

Interval: Sections 210-1276A-102R-1, 2 cm, through 75R-3, 142 cm

Depth: 1732.12–1502.12 meters below seafloor (mbsf)

Two sills intruded the sedimentary sequence of Subunit 5C (Subunit 5C2: interval 210-1276A-102R-CC through 97R-1 and Subunit 5C1: interval 88R-7, 122 cm, through 87R-6, 72 cm). The oldest sediments recovered comprise a sequence dominated by poorly organized green, gray, and black gravity flow deposits. These include sandy debris flow deposits and graded beds with abundant syndepositional deformation. In situ hemipelagic mudstone and claystone horizons are minor and are estimated to account for only ~10% of sediment recorded from Subunit 5C, with the remainder of the finest grained and calcareous material being deposited by mud-laden turbidity currents or debris flows (Tucholke, Sibuet, Klaus, et al., 2004). Evidence of burrowing is rare in this section but where present is largely confined to the hemipelagic mudstone intervals. Rare black shale horizons, identified by their very thin laminations (<1 mm), nannofossil abundance, and high total organic carbon (TOC) content (>1 wt% TOC) represent <1% of the succession in Subunit 5C. Black shale horizons identified as Oceanic Anoxic Event 1b (OAE1b) are recorded in Cores 210-1276A-95R and 94R. The top of this subunit is marked at 1502.12 mbsf by the first upsection appearance of disorganized beds of silty and muddy sandstone.

These predominantly dark mudrock sediments yield microfossil assemblages consistent with an early to middle Albian age. The stratigraphically lowest sample containing nannofossils is Sample 210-1276A-97R-1, 46–47 cm. This strongly depauperate assemblage is affected by dissolution and hence it is not reliable for a chronologic attribution of the very base of the section. The lowest datable sample is 210-1276A-96R-5, 92–93 cm, which is likely earliest Albian in age. It contains a poorly preserved yet abundant assemblage characterized by occurrences of *Prediscosphaera columnata* (subcircular to circular mor-

phototypes; see discussion by Bown in Kennedy et al., 2000), *Prediscosphaera spinosa*, *Rucinolithus irregularis/albiensis*, *Cylindralithus nudus*, *Helicolithus trabeculatus*, *Braarudosphaera batilliformis*, and *Eiffellithus? hancockii*. This assemblage indicates Subzone NC8a, which spans the uppermost Aptian and lowermost Albian. The first occurrences (FOs) of *P. columnata* (subcircular to circular morphotypes), *C. nudus*, and *H. trabeculatus* were reported from uppermost Aptian sediments of the French Vocontian Basin (*plesiotypica/jacobi* ammonite zone; Kennedy et al., 2000). The FO of circular *P. columnata* is often used as a proxy marker for the Aptian/Albian boundary in the literature (see Bown in Kennedy et al., 2000, for a synthesis). Sample 210-1276A-95R-5, 116–117 cm, contains *Lithraphidites alatus*, a taxon that is generally reported from Albian sediments and has never been reported from upper Aptian sediments. The difficulty in distinguishing zonal marker *Hayesites albiensis* from *Hayesites irregularis* due to dissolution complicates the recognition of lower Albian Subzone NC8b. The first *H. albiensis* was recognized in Sample 210-1276A-94R-5, 136–137 cm, but stratigraphically higher occurrences are spotty. However, because of the poor preservation of the calcareous nannofossil assemblages and the spotty occurrences of *H. albiensis*, an undifferentiated Subzone NC8a–NC8b is used for the biostratigraphy of Cores 210-1276A-96R through 77R.

Laminated black shales in Cores 210-1276A-95R and 94R are also characterized by high abundances of *Biscutum constans*, *Discorhabdus rotatorius*, and small *Zeugrhabdotus* spp.

The stratigraphically lowest planktonic foraminifers were found in Sample 210-1276A-94R-6, 55–58 cm (Leckie and Urquhart, unpubl. data). The very rare but moderately well preserved specimens occur in a sandy turbidite within the laminated black shale interval spanning nearly all of Cores 210-1276A-94R and 95R. Based on the presence of *Hedbergella* cf. *H. rischi* and the absence of diagnostic Aptian taxa, this black shale interval is assigned an earliest Albian age (*Hedbergella planispira* Zone KS12) in agreement with the nannofossil age assignment.

Small specimens of the calcareous nannofossil *Tranolithus* (*T. praeorionatus*, Bown in Kennedy et al., 2000) occur as low as Sample 210-1276A-81R-4, 60–61 cm. These transitional forms can be distinguished on the basis of their small size (<5 µm). The reliability of *Tranolithus orionatus* as a biostratigraphic marker in the lower middle Albian depends on the recognition of these morphotypes. The FO of regular morphotypes of *T. orionatus* in Sample 210-1276A-77R-3, 51–52 cm (1521.65 mbsf), represents the lower boundary of middle Albian Subzone NC8c.

The interval from Cores 210-1276A-97R through 81R is nearly barren of planktonic foraminifers apart from rare to few specimens in samples between intervals 83R-1, 51–55 cm, and 78R-3, 4–8 cm. These specimens are, very small and poorly preserved, and probably redeposited; therefore, no reliable age determinations are possible.

Other microfossils recovered from this interval lack age-index species and include common to abundant agglutinated foraminifers, common to abundant radiolarians, rare calcareous benthic foraminifers, and rare fish teeth. The assemblages of agglutinated benthic foraminifers are consistent with the Albian age determination and are representative of biofacies of a similar age recovered from other DSDP and ODP sites drilled in the North Atlantic and the Carpathians (Kaminski et al., 1999; Kuhnt and Urquhart, 2001). Radiolarian assemblages are also consistent in age with sediments deposited during Albian times with occurrences of characteristic species (Thurrow, 1988) Carbonized plant debris is consistently common throughout Subunit 5C with common

and abundant megaspores in two samples: 210-1276A-94R-4, 24–28 cm, and 94R-3, 128–132 cm.

Lithologic Subunit 5B

Age: middle Albian–early Cenomanian

Interval: Sections 210-1276A-75R-3, 142 cm, through 36R-2, 129 cm

Depth: 1502.12–1129.80 mbsf

This subunit consists of a sequence of dark-colored calcareous mudstone with a few minor debris flow horizons of calcareous siltstone and sandstone. The mudstones are quite extensively burrowed and have been interpreted as a series of hemipelagic sediments and mud turbidites. Occasional diagenetic nodules and concretionary bands of siderite, dolomite, barite, and pyrite are recorded. The mineral content of the washed residues (>38 μm) includes common mica, common pyrite, and abundant, well-sorted fine angular quartz grains throughout most of the section.

The interval between Samples 210-1276A-77R-3, 51–52 cm (1521.65 mbsf), and 69R-2, 118–119 cm, represents Subzone NC8c, the lower boundary of which occurs in Subunit 5C recorded above. The zonal marker for lower middle Albian Subzone NC8c, *T. orionatus*, is also present in Sample 210-1276A-69R-5, 102–103 cm. The occurrence of *Axopodorhabdus albianus* in Sample 210-1276A-69R-2, 118–119 cm, indicates middle Albian Subzone NC9a. Samples 210-1276A-53R-6, 46–47 cm (1300.47 mbsf), through 45R-5, 110–111 cm (1223.48 mbsf), are placed in Subzone NC9b based on the FO of *Eiffellithus monechiae* found in the former sample.

Cores 210-1276A-48R through 45R are assigned to upper Albian *Rotalipora ticinensis* Zone KS15 based on the presence of *R. ticinensis*, *Rotalipora subticinensis*, *Ticinella roberti*, *Ticinella primula*, *Biticinella breggiensis*, and *Globigerinelloides bentonensis*. Cores 210-1276A-45R through 41R are assigned to the uppermost Albian *Rotalipora appenninica* Zone KS16. Age-diagnostic species include *R. appenninica*, *R. ticinensis*, *Planomalina buxtorfi*, *Praehedbergella delrioensis*, and *Hedbergella libyca*.

Uppermost Albian sediments, zoned as Subzone NC10a based on the FO of *Eiffellithus turriseiffelii*, were encountered in Sample 210-1276A-45R-3, 130–141 cm (1220.06 mbsf), and persist through Sample 37R-3, 96–97 cm (1140.12 mbsf). The calcareous nannofossil species *Corollithion kennedyi*, which approximates the base of the Cenomanian for the purpose of this study, is found in Sample 210-1276A-37R-1, 102–103 cm (1137.42 mbsf) together with *Lithraphidites acutus*, thus indicating mid-Cenomanian Zone UC3. The lower Cenomanian biozones UC1 and UC2 are missing.

A thin section from Section 210-1276A-36R-2 is assigned to the lower Cenomanian *Rotalipora globotruncanoides* Zone KS17 based on the presence of *R. globotruncanoides*, *R. appenninica*, *Praeglobotruncana delrioensis*, *Praeglobotruncana stephani*, and *H. libyca*. The presence of the latter taxon suggests that this sample lies in the basal Cenomanian due to the presence of *H. libyca*, which characterizes a narrow zone straddling the Albian–Cenomanian boundary interval (Leckie, 1984; Bellier et al., 2000). Therefore, the Albian/Cenomanian boundary occurs between Cores 210-1276A-41R and 36R according to the planktonic foraminifers.

Other microfauna recovered from samples in Subunit 5B include consistently common and abundant occurrences of agglutinated foraminifers up to Sample 210-1276A-39R-1, 41–45 cm. Above this horizon, although these benthic forms consistently occur, their numbers are much reduced and rare occurrences are recorded. Calcareous benthic foraminifers are present throughout the section but are very small, size-sorted specimens and are considered to be reworked from shallower parts of the continental margin. Radiolarians occur in common and abundant numbers throughout the section and are usually very small (<125 µm) and pyritized. Wood and plant debris become rare and sporadic above Sample 210-1276A-51R-4, 66–70 cm.

Lithologic Subunit 5A

Age: Cenomanian–Turonian

Interval: 210-1276A-36R-2, 129 cm, through 29R-6, 62 cm

Depth: 1129.80–1067.24 mbsf

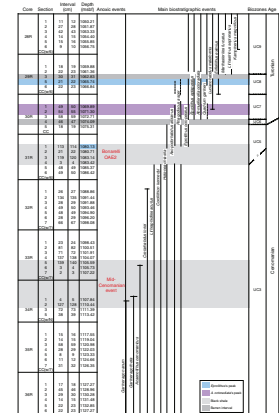
Lithologic Subunit 5A is dominated by thick, graded gravity flow deposits of greenish gray calcareous sandstone, minor grainstone, and unlaminated calcareous mudstone. The sediments are only moderately burrowed. Black shale horizons identified as OAE 2 are recorded in Sections 210-1276A-31R-4, 31R-3, and 31R-2 and are completely devoid of burrowing.

Cores 210-1276A-36R through 35R contain a good succession of lower Cenomanian calcareous nannofossil biostratigraphic events including the LOs of *Gartnerago theta* in Sample 210-1276A-36R-5, 22–23 cm, *Gartnerago nanum* in Sample 36R-4, 14–15 cm, and *Cretarhabdus loriei* in Sample 35R-7, 31–32 cm.

The “Mid-Cenomanian Event” (Coccioni and Galeotti, 2003) was recognized between Cores 210-1276A-34R and 33R. This event lies in nannofossil Zone UC3. The calcareous nannofossil species *G. theta* and *G. nanum* disappear in this interval (Sections 210-1276A-34R-1 and 34R-2, respectively) (Fig. F4), as does *Acaenolithus cenomanicus* (Section 33R-6). These nannofossil events were used by Burnett (1998) to further subdivide Zone UC3; however, their stratigraphic order differs from that indicated by the author and no subzonal divisions were applied.

Cores 210-1276A-32R through 31R contain a succession of uppermost Cenomanian through lower Turonian calcareous nannofossil biostratigraphic events (Fig. F4): *C. loriei* (= *C. striatus*) last occurs in Sample 210-1276A-32R-1, 26–27 cm; *L. acutus* and *C. kennedyi* vanish in the barren samples representing the Bonarelli Level (OAE2) (Sections 210-1276A-31R-4 to 31R-1). This barren interval might contain the uppermost part of Zone UC3, Zone UC4, and much of Zone UC5. *Eiffellithus* cf. *E. eximius* was sporadically observed in Sample 210-1276A-31R-6, 49–50 cm. This latter species seems to be a transitional morphotype from *E. turriseiffelii* to *E. eximius*, a marker species of the middle Turonian (Bralower, 1988; Watkins et al., 1993). Sample 210-1276A-31R-1, 113–114 cm, contains some specimens of *Quadrum intermedium* (six and five rays), and it is also characterized by a high abundance of *Eprolithus* spp., (first *Eprolithus* peak) (Fig. F4), particularly *Eprolithus octopetalus*. The first occurrence of *E. octopetalus* is reported as an early Turonian event in the recent literature (UC5 biozone, Burnett, 1998; Bralower and Bergen, 1998; Luciani and Cobianchi, 1999) although Perch-Nielsen (1979) indicated a late Cenomanian FO for this species.

F4. Cenomanian–Turonian calcareous nannofossil bioevents, p. 44.



The upper Cenomanian *Rotalipora cushmani* Zone KS19 is recognized in a thin section from Section 210-1276A-31R-5 based on the presence of *R. cushmani* and *Whiteinella archeocretacea*. Thin sections from Sections 210-1276A-31R-1 and 30R-5 are assigned to the uppermost Cenomanian–lowermost Turonian *W. archeocretacea* Zone KS20 based on the presence of the nominate taxon together with *Dicarinella* cf. *D. caniculata* and *Praeglobotruncana* cf. *P. praehelvetica*.

Sample 210-1276A-30R-3, 54–55 cm, contains the FOs of calcareous nannofossils *Quadrum gartneri*, *Eprolithus eptapetalus*, and *Ahmuellerella octoradiata*, thus indicating that much of Zone UC6 is reduced based on the absence of the expected succession of bioevents (Fig. F4). Sample 210-1276A-29R-CC is assigned to middle to upper Turonian Zone UC8 based on the presence of *Eiffellithus eximius*. According to planktonic foraminifer evidence, Sample 210-1276A-29R-CC is likely late early Turonian to early late Turonian age (*Helvetoglobotruncana helvetica* Zone KS21) based on the co-occurrence of *Marginotruncana renzi*, *Marginotruncana sigali*, *Dicarinella imbricata*, *P. praehelvetica*, and *Whiteinella aprica*. However, planktonic foraminifers are very rare and poorly preserved in this sample.

Sample 210-1276A-29R-6, 22–23 cm, contains abundant *Eprolithus* spp. (second *Eprolithus* peak), but the higher abundances are recorded by *E. eptapetalus*. Sample 210-1276A-29R-2, 22–23 cm, is placed in the uppermost Turonian Zone UC9 based on the co-occurrence of *E. eximius*, *Marthasterites furcatus*, and *Lithastrinus septenarius*. Samples 210-1276A-28R-CC and 28R-5, 76–77 cm, contain a rather depauperate assemblage assigned to uppermost Turonian–lower Coniacian Zone UC9, based on the absence of *Broinsonia* spp., *Arkhangelskiella cymbiformis*, and *Micula decussata* and the presence of *E. eximius*, *Q. gartneri*, *L. septenarius*, *M. furcatus*, and *Kamptnerius magnificus*.

Radiolarians are generally not preserved in the sediments of Subunit 5A, although they do occur commonly in two samples, once just below the OAE2 interval in Sample 210-1276A-33R-CC and once just above the event in latest Cenomanian–earliest Turonian Sample 31R-4, 8–12 cm.

Lithologic Unit 4

Age: Turonian–Campanian

Interval: 210-1276A- 29R-6, 62 cm, through 25R-5, 80 cm

Depth: 1067.24–1028.00 mbsf

The dominant siliciclastic Turonian to Campanian lithologies of the section assigned to Unit 4 are reddish brown bioturbated muddy sandstone and sandstone and have been distinguished primarily by the intensity of burrowing together with the color and grain size of the sediments.

Sections between 210-1276A-28R-5 and 25R-6 are barren of calcareous microfossils. Many samples were taken from different lithologies in this thick interval in an attempt to constrain the age, but none yielded nannofossils. It is inferred that the interval contains all of the calcareous nannofossil zones between upper Coniacian Zone UC10 and mid-Campanian Zone UC15; the latter zone is recognized in Sample 210-1276A-25R-5, 25–26 cm, by the occurrence of *Uniplanarius sissinghi* and *Uniplanarius trifidus* together with *Reinhardtites anthophorus* and *E. eximius*.

The fact that these samples are barren of in situ age-diagnostic calcareous microfossils is considered to be a likely consequence of an elevated CCD during the Late Cretaceous (Thierstein, 1979; Tucholke and Vogt,

1979). A few specimens of planktonic foraminifers have been recovered from Core 210-1276A-27R but they are very small and poorly preserved. Recovery of agglutinated foraminifers from Unit 4 is also poor, although Sample 210-1276A-25R-4, 87–91 cm, yielded a moderately diverse assemblage of these forms. Rare radiolarians and rare fish teeth are also present in these Turonian–Campanian sediments.

Lithologic Unit 3

Age: mid-Campanian–Paleocene
Interval: 210-1276A-25R-5, 80 cm, through 15R-3, 125 cm
Depth: 1028.00–929.25 mbsf

This unit consists predominantly of reddish brown calcareous mudstone with minor horizons of gray calcareous siltstone and sandstone. Gravity flow deposits of mud-dominated turbidites are common, and burrow structures, although present, are restricted to the uppermost few tens of centimeters of these deposits.

Campanian–Maastrichtian

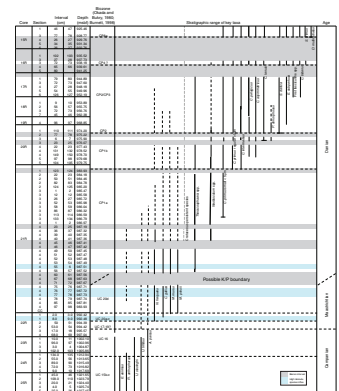
Mid-Campanian Zone UC15 is recognized from Sample 210-1276A-25R-5, 25–26 cm, to 24R-2, 55–56 cm, where the last *E. eximius* is observed (Fig. F5). The next sample, 210-1276A-24R-1, 134–135 cm, contains very rare *R. anthophorus* and abundant *Reinhardtites levis*, an abundance crossover that will characterize the entire upper Campanian Zone UC16. *U. sissinghi* and *U. trifidus* are observed through the top of Core 210-1276A-23R (Fig. F5). Sections 210-1276A-22R-4 and 22R-3 contain the upper part of Biozone UC16, the last *Aspidolithus parvus* being observed in Sample 210-1276A-22R-3, 17–18 cm. The Campanian/Maastrichtian boundary is placed between Sections 210-1276A-22R-4 and 22R-3 (Fig. F5).

It is likely that much of the Maastrichtian at this site is condensed in Core 210-1276A-22R based on calcareous nannofossil evidence. The assemblage in Sample 210-1276A-22R-2, 50 cm, is characterized by the absence of *Lithraphidites quadratus* and *T. orionatus*, which could indicate undifferentiated mid-Maastrichtian Zones UC19–UC18. Sample 210-1276A-22R-1, 2 cm, indicates the presence of upper Maastrichtian Subzones UC20a–UC20c based on the lack of *Micula murus* and the presence of common *L. quadratus*, *Cribracorona gallica*, *A. cymbiformis*, and *Nephrolithus frequens*. Sample 210-1276A-21R-CC yields a poorly preserved assemblage that is characterized here as upper Maastrichtian Zone UC20 based on the presence of *M. murus* and *Micula prinsii*.

The uppermost Campanian and upper Maastrichtian assemblages are characterized by typical low-latitude Tethyan taxa such as *U. trifidus* and *L. quadratus* mixed with cooler-water high-latitude species such as *Cribrosphera daniae* and *Psyktoisphaera firthii*. *N. frequens*, the marker taxon of upper Maastrichtian Zone CC26 (Sissingh, 1977), is common, whereas the tropical species *M. murus* (a marker for this zone at low latitudes) is very rare at Site 1276. These data suggest that Site 1276 occupied an intermediate region between the Boreal and Tethyan provinces and that mixed assemblages were common during this time period.

A late Campanian age is suggested for Core 210-1276A-24R (*Globotruncana aegyptiaca* Zone KS29 or lower *Gansserina gansseri* Zone KS30) based on the presence of *Globotruncana ventricosa* and *G. aegyptiaca* and the absence of *Globotruncana falsostuarti* and *Globotruncanita*

F5. Mid-Campanian to early Paleogene calcareous nannofossil bioevents, p. 45.



calcarata. The occurrence of *Globotruncana* cf. *G. falsostuarti* in Sample 210-1276A-22R-CC suggests the presence of the lower Maastrichtian part of the *G. gansseri* Zone KS30. The lower part of Core 210-1276A-21R is assigned to the upper Maastrichtian *Abathomphalus mayaroensis* Zone KS31 based on the presence of the nominate taxon and a moderately diverse assemblage of globotruncanids and rugoglobigerinids.

Cretaceous/Paleogene (K/P) Boundary

Determining the position of the Cretaceous/Paleogene (K/P) boundary transition in Hole 1276A with calcareous nannofossils was difficult because of extensive reworking and the presence of several intervals of carbonate-free sediments.

In several low-latitude and Atlantic localities that contain a biostratigraphically continuous transition between the uppermost Maastrichtian and the lowermost Danian, the K/P boundary is marked by peculiar biotic changes in the calcareous nannoplankton community (Gardin and Monechi, 1998, and references therein). These changes include the following: the lowest Danian sediments are characterized by a dramatic increase in the abundance of the calcareous dinocyst *Thoracosphaera* spp. (“*Thoracosphaera acme*”), occurring together with a lowered abundance of Cretaceous species that are assumed to be reworked. This “bloom” of *Thoracosphaera* spp. is followed by an increase in abundance of survivor coccolith species such as *Markalius inversus*, *Cyclagelosphaera reinhardtii*, *Braarudosphaera bigelowii*, *Zeughrabdodus sigmoides*, *Neocrepidolithus* spp., and holococcoliths such as *Octolithus multiplus* and *Lanternithus minutus*. These coccoliths are usually very rare in late Maastrichtian assemblages but they increase in abundance in the aftermath of the K/P crisis. Blooms of dwarf coccolith species such as *Neobiscutum romeinii* and *Neobiscutum parvulum* are also a typical feature of early Danian assemblages. The more complex Danian species, *Cruciplacolithus primus*, appears during this time and rapidly increases in size (the first specimens are <5 µm) and abundance (Gardin and Monechi, 1998). At higher latitudes, the first occurrence of *Biantholithus sparsus* in lowest Danian sediments is usually used as a proxy for the K/P boundary (Gartner, 1996).

All of these biotic signals were instrumental in constraining the K/P boundary transition in Hole 1276A to Section 210-1276A-21R-4 (Fig. F5). Samples 210-1276A-21R-4, 103–104 cm, 21R-4, 97–98 cm, and 21R-4, 77 cm, contain abundant and diverse uppermost Maastrichtian assemblages belonging to the *M. prinsii* Subzone UC20d. The assemblages are characterized by common occurrences of “cool-water taxa” such as *K. magnificus*, *N. frequens*, and *P. firthii*, indicating cooler surface waters prior to the boundary, as also found worldwide. Sample 210-1276A-21R-4, 77 cm, also contains high abundances of *Prediscosphaera stoveri*, whose acme is considered as a latest Maastrichtian feature in the Atlantic domain (Jiang and Gartner, 1986; Thibault and Gardin, 2006). These samples are followed by a first barren interval (Samples 210-1276A-21R-4, 71 cm, 21R, 67 cm, and 21R-4, 70 cm) (Fig. F5). Sample 210-1276A-21R-4, 56–57 cm, from a dark brownish green clay layer at the top of this barren interval, yields very rare Cretaceous species such as *M. decusata* and *Watznaueria barnesiae* together with several fragments of *Thoracosphaera* spp. Samples 210-1276A-21R-4, 53 cm, 21R-4, 51 cm, and 21R-4, 49 cm, from the carbonate turbidite overlying this clay layer, contain abundant and diverse Maastrichtian assemblages with no apparent Danian biotic components. The assemblages are characterized

by common occurrences of “cool-water taxa” as well as the acme of *P. stoveri* as observed in previous samples (210-1276A-21R-4, 103–104 cm, 21R-4, 97–98 cm, and 21R-4, 77 cm).

Another barren interval occurs at 210-1276A-21R-4, 45–47 cm. The overlying samples (210-1276A-21R-4, 41 cm, 21R-4, 40 cm, and 21R-4, 37 cm) still contain abundant Maastrichtian species but also contain many thoracosphaerid fragments and very abundant *N. parvulum* and *N. romeinii*. Coccoliths known to be true survivors (see text above) are also quite common, despite the great abundance of other Cretaceous species. According to these findings these latter samples bear the most convincing evidences of an early Danian age. Finally, *C. primus* (early forms <5 µm) was first encountered in Sample 210-1276A-21R-3, 113–114 cm (Fig. F5).

A thin section from interval 210-1276A-21R-4, 19–21 cm, contains common small planktonic foraminifers indicative of basal Paleocene Zone P α , including *Guembelitra cretacea*, *Parvularugoglobigerina eugubina*, and *Woodringina* sp., as well as the calcareous dinoflagellate *Thoracosphaera* against a backdrop of abundant reworked Late Cretaceous planktonic foraminifers.

Lower Paleocene

Following the K/P boundary transition, the lower Paleocene calcareous nannofossil succession of Hole 1276A can be summarized as follows (Fig. F5): Sections 210-1276A-21R-3 and 21R-2 are zoned as CP1a because of the presence of *C. primus* together with abundant thoracosphaerid fragments and Cretaceous survivor species such as *Z. sigmoides*, *M. inversus*, *Markalius panis*, and *C. reinhardtii*, some of them being very common in particular levels. Cretaceous species are still abundant, but the Paleogene species became progressively dominant in the upper part of Section 210-1276A-21R-2.

Section 210-1276A-21R-1 is barren and the base of Subzone CP1b is found immediately above, in Sample 210-1276A-20R-5, 105–106 cm, which is characterized by common *C. primus* (both small and regular morphotypes) and *Cruciplacolithus intermedius*, together with *Neocrepidolithus* sp., *M. inversus*, and thoracosphaerid fragments. *Coccolithus pelagicus* and *Cruciplacolithus asymmetricus* are first encountered in Sample 210-1276A-20R-4, 149 cm, associated with early morphotypes of *Cruciplacolithus tenuis*. The regular morphotypes of the latter species together with the FO of *Cruciplacolithus edwardsii* and the common occurrence of *Prinsius dimorphosus* were found in Sample 210-1276A-20R-3, 6–7 cm. Finally, the marker species for the base of Zone CP2, *Sullivania danica*, first occurs in Sample 210-1276A-20R-1, 110–111 cm. The lower Danian calcareous nannofossil succession found in Hole 1276A is comparable to other lower Danian successions found at different latitudes, including the Atlantic domain (Galbrun and Gardin, 2004), the North Sea (Van Heck and Prins, 1987; Varol, 1989), and Denmark (Perch-Nielsen, 1985), although the succession of some secondary markers does not exactly follow the same stratigraphic order.

Core 210-1276A-19R is attributed to Zone CP2 because of the occurrence of *Ericsonia subpertusa* in Sample 210-1276A-19R-4, 96–97 cm, *Prinsius tenuiculum*, *Prinsius martinii*, *Toweius* spp., and *Neochiastozygus modestus* in Sample 210-1276A-18R-7, 45–46 cm, and the absence of *Ellipsolithus macellus*, the marker for mid-Paleocene Zone CP3. The latter species was not encountered until Core 210-1276A-15R. *E. macellus* is known to be dissolution prone; however, its occurrence in very depau-

perate and etched assemblages such as those found in Core 210-1276A-15R (see below) might suggest that an ecological control also played a role in causing its absence.

Core 210-1276A-18R is assigned to an undifferentiated Zone CP2–CP3 based on the absence of any *Fasciculithus* species and the presence of *S. danica*, *E. subpertusa*, and *P. martinii*. The calcareous nannofossil assemblages that characterize Core 210-1276A-18R are scanty and poorly preserved; their chronologic reliability is therefore low. Very rare fasciculiths (*Fasciculithus ulii*, *Fasciculithus magnicordis*, and *Fasciculithus magnus*) and *Bomolithus elegans* were first observed in Sample 210-1276A-17R-6, 125–126 cm, together with *Chiasmolithus bidens*; *Neochiastozygus perfectus* was encountered in Sample 17R-1, 79–80 cm. The occurrence of these nannofossil species and the lack of *Fasciculithus tympaniformis* might indicate the Danian/Selandian Zone CP3.

Thin sections from Section 210-1276A-18R-6 contain the planktonic foraminifer *Parasubbotina pseudobulloides*, suggesting an early Paleocene age (undifferentiated Zones P1–P2). The presence of *Morozovella conicotruncana* in Section 210-1276A-17R-4 indicates lower upper Paleocene Zone P3.

The lower part of Core 210-1276A-16R is totally barren of nannofossils (Samples 16R-5, 79–80 cm, and 16R-4, 65–66 cm), but Sample 16R-3, 72–73 cm, contains an abundant assemblage characterized by the occurrence of very common *C. bidens*, *N. perfectus*, *Sphenolithus primus*, *F. ulii*, *Fasciculithus bitectus*, and very rare *Heliolithus cantabriae*. The first occurrence of the latter species is known as a Zone CP4 event, although the marker species for this zone, *F. tympaniformis*, was not encountered.

The upper part of Core 210-1276A-16R (Sample 16R-3, 27–28 cm) and the lower part of Core 15R (Samples 15R-6, 26–27 cm, 15R-5, 34–35 cm, and 15R-4, 26–27 cm) are barren of nannofossils.

Lithologic Unit 2

Age: Paleocene–Eocene

Interval: 210-1276A-15R-3, 125 cm, through 8R-5, 113 cm

Depth: 929.25–864.73 mbsf

The sedimentary succession assigned to lithologic Unit 2 is represented by reddish brown and yellowish green calcareous mudstones interbedded with yellowish and greenish gray calcareous siltstones and sandstones. Graded bedding and partial Bouma sequences support the interpreted presence of turbiditic deposits.

Upper Paleocene

Samples 210-1276A-15R-3, 77–78 cm, and 15R-1, 45–46 cm, contain depauperate and strongly etched assemblages, but *E. macellus*, *F. tympaniformis*, *Heliolithus kleinpellii*, *Heliolithus riedelii*, *Chiasmolithus consuetus*, and *Discoaster multiradiatus* could be recognized, allowing us to assign upper Paleocene Subzone CP8a to this interval. Substantial parts of Zone CP4 and Zones CP5–CP7 are thus missing because of a strongly condensed interval (hiatus?) spanning the upper part of Core 210-1276A-16R and the lower part of Core 15R.

Section 210-1276A-15R-1 is assigned to upper Paleocene Zone P4 based on the presence of the planktonic foraminifer zonal marker species *Globanomalina pseudomenardii*. Sample 210-1276A-14R-CC is assigned to upper Paleocene Subzone P4c based on the co-occurrence of *G. pseu-*

domenardii, *Morozovella aequa*, and *Igorina albeari*. Preservation is generally moderate, and whole specimens are filled with calcite. Abundant and well-preserved reworked Late Cretaceous (Campanian–Maastrichtian) planktonic foraminifers are noted in samples from Cores 210-1276A-14R and 9R.

Paleocene/Eocene Boundary

The Paleocene/Eocene (P/E) boundary is characterized by a brief (<250 k.y.) (Röhl et al. 2000) and abrupt worldwide warming event often referred to as the Paleocene/Eocene Thermal Maximum (PETM) and a concomitant perturbation of the global carbon budget. In the supra-CCD oceanic sedimentary record, the PETM interval typically corresponds to a sharp lithologic change uphole from light calcareous marl to a dark clayey, calcite-free dissolution interval a few centimeters to decimeters thick. This interval is also distinguished by a sharp negative $\delta^{13}C$ excursion (CIE), a benthic foraminiferal extinction event (BFEE) (Zachos et al., 2001; Thomas and Shackleton, 1996), and a reorganization of surface-dwelling communities (Kelly et al., 1996; Bralower, 2002).

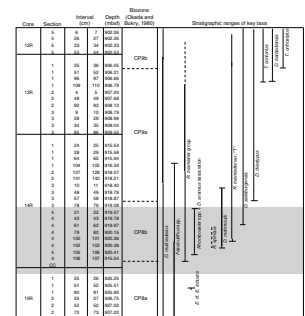
Biostratigraphically, the PETM lies at the top of calcareous nannofossil Zones CP8 and NP9 of Okada and Bukry (1980) and Martini (1971), respectively.

At the Paleocene–Eocene transition and during the PETM, the calcareous nannoplankton community shows a turnover characterized by peculiar biotic changes: the first members of the *Rhombaster-Tribrachiatus* lineage evolve and radiate just above the dissolution interval in association with “deformed discoasters” (*Discoaster araneus* and *Discoaster anartios*). This event is accompanied by a sharp decrease in abundance of the Paleocene genus *Fasciculithus* counterbalanced by an increase in *Zygrhablithus bijugatus* abundance (Bralower et al., 1995b; Tremolada and Bralower, 2004; Raffi et al., 2005). During this time interval until the recovery, the calcareous nannofossil assemblages are characterized by abundant and diverse *Discoaster* species, while the genera *Chiasmolithus*, *Prinsius*, and *Toweius* spp. are virtually excluded.

Identification of the Paleocene/Eocene boundary at Site 1276 was difficult for two main reasons: (1) the presence of several clayey calcite-free intervals deposited below the CCD and (2) the occurrence of turbidites and debris flows, which blur the typically distinct lithologic and paleontological record, specifically, the absence of a single dissolution interval and the reworking of key taxa. The placement of the PETM and the P/E boundary at Site 1276 was assigned using data from samples spanning the interval from Sections 210-1276A-15R-3 through 12R-5, 6–7 cm (Fig. F6). The upper part of Core 210-1276A-15R (Sections 15R-3 through 15R-1) is characterized by abundant and fairly well preserved assemblages belonging to the upper part of Subzone CP8a (occurrence of *D. multiradiatus*, *Discoaster nobilis*, abundant and diverse fasciculithids such as *Fasciculithus alanii*, *F. bitectus*, *Fasciculithus schaubii*, *Fasciculithus tonii*, *Fasciculithus thomasii*, and *Sphenolithus anarrhopus* and lack of *Ericsonia robusta* and *Rhombaster* spp.). Sample 210-1276A-14R-CC contains a poorly preserved yet diverse assemblage of nannofossils, including common fasciculithids and very rare *Rhombaster* spp. belonging to the “cube-shaped” specimens described by Angori and Monechi (1996).

Almost all of the remaining samples from Core 210-1276A-14R are characterized by poorly preserved, low-diversity, and low-abundance as-

F6. Calcareous nannofossil bio-events, p. 46.



semblages. However, these samples do contain important nannofossil biostratigraphic events that help to better constrain the PETM at Site 1276 (Fig. F6). The lowest sample of Section 210-1276A-14R-4 (14R-4, 106–107 cm) is characterized by the occurrence of the *Rhomboaster bramlettei* group (both morphotypes with “long” and “short” arms; see Angori and Monechi, 1996 for discussion) and is assigned to Subzone CP8b. Common *R. bramlettei* associated with *D. araneus* characterizes the assemblages from Sample 210-1276A-14R-4, 106 cm, to 14R-4, 21–22 cm. *Rhomboaster spineus* and *Discoaster mahmoudii* occur in Sample 210-1276A-14R-4, 102 cm, to 14R-4, 61–62 cm, and 14R-3, 48 cm, respectively. The morphotype *R. bramlettei* var. “T” (Angori and Monechi, 1996) was first encountered in Sample 210-1276A-14R-4, 100 cm. Other important FOs are *Discoaster salisburgensis* in Sample 210-1276A-14R-4, 79–80 cm, and *Discoaster diastypus* (side-view specimens) in Sample 14R-1, 24–25 cm, which marks the base of Subzone CP9a. The FO of *Tribrachiatus contortus* is in Sample 210-1276A-13R-1, 109 cm. The FO of *Tribrachiatus orthostylus* occurs in Sample 210-1276A-13R-1, 35 cm, indicating lowest Eocene Subzone CP9b.

The samples from Core 210-1276A-13R contain low-abundance and low-diversity assemblages dominated by abundant *Discoaster* species (*D. multiradiatus* being the most abundant species), with common *R. bramlettei* and *Sphenolithus moriformis*, whereas *C. pelagicus*, *Toweius* spp., and *Chiasmolithus* spp. are virtually excluded. This exclusion is most likely ecologically driven and not a result of preferential preservation. These assemblages are not indicative of stability and suggest that surface water conditions remained warm and oligotrophic in the latest part of the PETM (occurrence of K-specialist *Discoaster*, *Sphenolithus*, and *Rhomboaster*; Bralower, 2002), as previously outlined by other authors (Monechi et al., 2000; Bralower, 2002; Tremolada and Bralower, 2004).

Two important biotic signals close to the P/E transition characterize the assemblages of several sites in the North and South Atlantic Ocean, Indian Ocean, and northwest Pacific Ocean. These are (1) a *Thora-cosphaera* peak (Raffi et al., 2005) just above the dissolution interval, followed by (2) a *Fasciculithus* spp./*Z. bijugatus* abundance crossover (Tremolada and Bralower, 2004; Raffi et al., 2005). A detailed quantitative analysis has not yet been performed to confirm or invalidate these features at Site 1276; however, the demise of genus *Fasciculithus* is confirmed from Samples 210-1276A-14R-3, 78–79 cm, through 13R-3, 85–86 cm; above this, *Fasciculithus* spp. are virtually excluded from assemblages and *F. tympaniformis* was not observed above Sample 14R-1, 104–105 cm. *Z. bijugatus* is quite common in Sections 210-1276A-14R-4 and 14R-3 but rare and even absent in Sections 13R-3 and 13R-2. It becomes common again in Section 210-1276A-13R-1.

The recovered sediments of Sections 210-1276A-14R-1 through 14R-4 contain a stratigraphically coherent succession of calcareous nannofossil events comparable to that observed at the PETM of other Atlantic localities. It is important to note, however, that the succession of biotic events found at Site 1276 is characteristic of the postdissolution interval immediately after the PETM; it is therefore possible that the interval not recovered between Samples 210-1276A-14R-CC and 14R-4, 105–106 cm, contains much of the dissolution interval. Alternatively, the uppermost Paleocene may be missing due to a hiatus at Site 1276 based on the planktonic foraminifer upper Paleocene Zone P4c assignment of Sample 210-1276A-14R-CC and the overlying succession of basal Eocene nannofossil events described from Sections 14R-1 through 14R-4.

Lower Eocene to Lower Middle Eocene

Sample 210-1276A-13R-CC contains only rare specimens of *D. multi-radiatus*, and Sample 12R-CC is barren of nannofossils. Sample 210-1276A-12R-4, 55 cm, may be constrained to lower middle Eocene Zone CP10 based on few specimens of *T. orthostylus*. Samples from 210-1276A-11R-CC through 8R-CC yield fairly abundant and moderately to poorly preserved assemblages. Samples 210-1276A-11R-CC and 10R-CC are assigned to the undifferentiated Zones CP10–CP11 based on the presence of *Discoaster lodoensis* in the absence of *Discoaster sublodoensis*. Zones CP10 and CP11 could not be differentiated because *Toweius crassus* was not observed in these sediments.

The absence of *Rhabdosphaera inflata* in Sample 210-1276A-9R-CC indicates Subzone CP12a. Subzone CP12a is delineated by the FO of *D. sublodoensis* in Sample 210-1276A-9R-5, 52–53 cm (Wood et al., submitted [N1]). Multiple specimens that closely resemble *D. sublodoensis* were noted in Samples 210-1276A-9R-5, 52–53 cm, through 9R-4, 23–24 cm, but are too overgrown to be positively identified. Subzone CP12b extends from Sample 210-1276A-8R-6, 100–101 cm, to 8R-6, 1–2 cm, based on the presence of *R. inflata*. Other notable species in this interval are *Cruciplacolithus cruciformis*, *D. lodoensis*, *D. sublodoensis*, *Discoaster tani nodifer*, *Neococcolithes dubius*, and *Sphenolithus radians*. A single specimen of *Chiasmolithus gigas* was recorded in Sample 210-1276A-8R-5, 131–132 cm. This specimen allows the delineation of Subzone CP13a; however, this boundary is tentatively placed (Table T1) because of the rare occurrence of the marker species.

T1. Biostratigraphic datums, p. 48.

Lithologic Unit 1

Age: middle Eocene–earliest Oligocene

Interval: 210-1276A-8R-5, 113 cm, through 8R-1, 50 cm

Depth: 864.73–753.00 mbsf

The sediments from Unit 1 are hemipelagic greenish brown mudstones interspersed with grainstones that exhibit planar lamination and are interpreted to be turbidites (Tucholke, Sibuet, Klaus, et al., 2004). The unit is predominantly a brownish color with shades of green and gray. The defining characteristics of Unit 1 are a high proportion of mudrock; disorganized deposits of muddy sandstone and sandy mudstone with pebble- and cobble-sized mudstone clasts; and a range of deformation features including normal faults, soft sediment folds, zones of ductile shearing, and crenulated lamination. The base of Unit 1 is placed at a sharp color and lithologic boundary at Section 210-1276A-8R-5, 113 cm. This horizon is situated near a middle Eocene hiatus and condensed interval (Wood et al., submitted [N1]). The mudrocks of Unit 1 are variably burrowed and represent slowly deposited hemipelagic sediments. The grainstones are normally graded and have planar lamination; they are interpreted as turbidites. The muddy sandstones and sandy mudstones form disorganized ungraded beds with scattered floating clasts of mudrock and marlstone, and they are interpreted as debris flow deposits. Grainstones in Unit 1 include a variety of carbonate and siliciclastic grains derived from shelf depths and deeper.

Shipboard analysis of calcareous nannofossils and organic-walled dinocysts suggested the presence of a disconformity within the lower middle Eocene (Tucholke, Sibuet, Klaus, et al., 2004). Wood et al. (submitted [N1]) suggest that the duration of the hiatus and condensed in-

terval is approximately 4.8 m.y. based on the FO of *R. inflata* in Sample 210-1276A-8R-CC (48.5 Ma) and the FO of *Reticulofenestra umbilica* in Sample 210-1276A-8R-5, 20–21 cm (43.7 Ma).

The interval from Sample 210-1276A-8R-5, 24–25 cm, through 8R-5, 131–132 cm, does not contain any stratigraphically useful species that may be used to subdivide this interval beyond Okada and Bukry (1980) Zones CP13b and CP13c. Typical assemblages in this interval generally contain rare to few specimens of *Chiasmolithus expansus*, *Chiasmolithus grandis*, *Chiasmolithus solitus*, *Coccolithus formosus*, *C. pelagicus*, *Reticulofenestra dictyoda*, *S. radians*, *Transversopontis pulcheroides*, and *Z. bijugatus*. However, reworked specimens of *R. dictyoda* occur sporadically above the FO of *R. umbilica*, which is noted in Sample 210-1276A-8R-5, 20–21 cm, and marks the base of Subzone CP14a.

Sample 210-1276A-7R-1, 26–27 cm, is placed in Subzone CP14b based on the LO of *C. solitus*. While samples above Sample 210-1276A-7R-1, 26–27 cm, may have their origin in Subzone CP14b as well and are certainly no older than CP14b, the mostly barren sediments and lack of age-diagnostic fossils make it impossible to ascertain a definite age for the interval from 210-1276A-6R-CC through the top of Core 4R (viewed at 4R-1, 126–127 cm).

Barren sections (green low- to no-carbonate mudstones) were predominant throughout Cores 210-1276A-7R through 4R. Calcareous nannofossils found in this interval are typically non-age-diagnostic species such as *C. formosus*, *C. pelagicus*, *Reticulofenestra scrippsae*, and *Reticulofenestra samodurovii* and are poorly preserved when present. The only exception is Sample 210-1276A-7R-5, 145–146 cm, a turbidite interval containing very abundant moderately preserved fossils with much greater diversity than the surrounding sediments. Common and abundant nannofossils in this sample are, in addition to the above, *Blackites rectus*, *C. expansus*, *C. solitus*, *Pemma basquensis*, *Pemma papillatum*, *R. dictyoda*, *T. pulcheroides*, and *Z. bijugatus*.

The shipboard data gathered for the uppermost three cores from Hole 1276A was reexamined postcruise in an effort to resolve the biostratigraphic discrepancies between the dinoflagellate cysts and the calcareous nannofossils reported in the Leg 210 *Initial Reports* (Tucholke, Sibuet, Klaus, et al., 2004). The interval from 210-1276A-3R-CC through the top of the core is generally populated by background fossils, with few to no marker species. Samples taken in Core 3R (210-1276A-3R-CC and 3R-2, 51–52 cm) are particularly difficult to date for this reason.

However, the concurrent LO of *M. inversus* and FO of *Clausicoccus subdistichus* in Sample 210-1276A-2R-CC indicate that this sample is likely placed in Subzone CP15b (34.2 Ma). This subzone extends through Sample 210-1276A-2R-1, 144–145 cm. Background assemblages in this horizon include *Blackites spinosus*, *Cyclicargolithus obrutus*, *Coccolithus* spp., *Discoaster deflandrei*, *Helicosphaera euphratis*, *L. minutus*, *Pontosphaera* spp., *Reticulofenestra* spp., *S. moriformis*, and *Z. bijugatus*. Multiple reworked species in this interval include *C. solitus*, *C. grandis*, *D. binodosus*, and *R. dictyoda* (original data from Tucholke, Sibuet, Klaus, et al., 2004).

The FO of *Chiasmolithus altus* in Sample 210-1276A-1W-CC allows for the delineation of Subzone CP16a, which includes Samples 210-1276A-1W-CC and 1R-4, 37–38 cm. This represents the highest section cored in Hole 1276A and includes specimens of *B. spinosus*, *C. altus*, *C. subdistichus*, *C. formosus*, *Cyclicargolithus floridanus*, *H. euphratis*, *L. minutus*, *Pemma* spp., *R. umbilica*, *Z. bijugatus*, and reworked specimens of

Discoaster saipanensis and *Reticulofenestra reticulata* (original data from Tucholke, Sibuet, Klaus, et al., 2004).

PALEOENVIRONMENTAL INTERPRETATIONS

Lithologic Subunit 5C

Age: early to middle Albian

Interval: 210-1276A-102R-1, 2 cm, through 75R-3, 142 cm

Depth: 1732.12–1502.12 mbsf

Cores 210-1276A-95R and 94R contain very common calcareous nanofossil fertility index species such as *D. rotatorius*, *Biscutum* spp., and *Zeugrhabdotus moulladei*, suggesting that the enriched organic matter in the laminated black shales is at least partially the consequence of elevated productivity. Cores 210-1276A-95R and 94R are also characterized by high abundances of *B. constans*, *D. rotatorius*, and small *Zeugrhabdotus* spp. These taxa are well known from the literature to be indicators of high fertility of surface waters (Roth and Bowdler, 1981; Premoli Silva et al., 1989; Coccioni et al., 1992; Erba et al., 1992).

This laminated black shale interval likely correlates with the “Niveau Paquier” black shale of the Vocontian Basin in southeast France (Bréhéret, 1994). Elsewhere it is known as OAE1b (e.g., Erbacher et al., 1996; Leckie et al., 2002). If so, this is one of the deepest-water examples of OAE1b known, and it is also one of the thickest (e.g., Erbacher et al., 1998, 1999, 2001). Nannofossil evidence shows that high-fertility conditions characterize the black shale interval.

No benthic foraminifers or other evidence of benthic organisms, including burrows, were found in the laminated black shale of OAE1b at Site 1276, suggesting that the deepest parts of the central North Atlantic were anoxic at this time. This finding complements data based on membrane lipids (biomarkers) extracted from organic matter preserved in an OAE1b black shale from the western North Atlantic suggesting that much of water column may have been anoxic during this event because of a massive expansion of chemoautotrophic Archaea (Kuypers et al., 2001).

The paucity of calcareous planktonic and benthic foraminifers recovered from sediments in Cores 210-1276A-97R through 75R suggests that the depositional environments were below the CCD and probably at abyssal depths and that the rare specimens recovered are actually a product of debris flows and turbidity currents. Relatively abundant and diverse assemblages of agglutinated foraminifers indicate that bottom conditions were possibly conducive to these assemblages, and, although generally small, the characteristic genera recovered are representative of deeper-water dwellers such as *Ammodiscus* spp., *Rhizammina* spp., and *Glomospira* spp. (Kuhnt and Urquhart, 2001). The distinct paucity of burrows indicates that conditions were not hospitable for all bottom-dwelling organisms.

The presence of abundant radiolarians throughout lithologic Subunit 5C between Samples 210-1276A-97R-4, 66–70 cm, and 76R-6, 118–122 cm, the rare but consistent occurrence of fish teeth, and the fact that calcareous nannofossils were present in surface waters suggest that surface waters and probably the upper part of the water column were subject to normal open-marine conditions during this interval.

Common wood and plant debris recovered consistently through this sedimentary subunit (1706.57–1502.12 mbsf) and throughout the Albian sediments until upper Albian Sample 210-1276A-51R-4, 66–70 cm, in Subunit 5B above, suggest that although the seafloor was at abyssal depths the site was exposed to strong influence from the adjacent land mass. It also suggests that the prevailing climate supported abundant vegetation and that there was sufficient run-off to transport large quantities of this material into the marine realm.

Lithologic Subunit 5B

Age: Albian–Cenomanian

Interval: 210-1276A- 75R-3, 142 cm, to 36R-2, 129 cm

Depth: 1502.12–1129.80 mbsf

The upper Albian at Site 1276 (Cores 210-1276A-48R through 41R) is characterized by moderately preserved and rare to moderately abundant assemblages of planktonic foraminifers. The greater abundance of planktonic foraminifers parallels generally higher concentrations of carbonate along continental margins during the late Albian, as well as larger sizes and more calcified species of planktonic foraminifers at this time (Leckie et al., 2002). A greater flux of carbonate associated with increased carbonate productivity in the near-surface ocean can buffer the carbonate solubility of the deep ocean, thereby enhancing carbonate preservation in an otherwise carbonate-poor environment (e.g., McCarthy et al., 2004). In addition to greater abundance and improved preservation, not all uppermost Albian assemblages of Site 1276 show the pronounced size sorting observed in the upper lower to lower upper Albian interval, therefore suggesting that the pelagic rain of carbonate reached the seafloor during latest Albian time.

Organic carbon-rich black shales in the upper Albian of Hole 1276A (Tucholke, Sibuet, Klaus, et al., 2004) may be correlative to other suspected OAEs (OAE1c in the upper Albian and OAE1d in the uppermost Albian) (Leckie et al., 2002; **Arnaboldi and Meyers**, this volume). These black shales may reflect times of enhanced productivity in surface waters and deposition under anoxic seafloor conditions. The abundance and small size of the radiolarian assemblages recovered could be indicative of enhanced productivity at the surface and upper reaches of the water column. Conversely, the limited size range of the specimens may be due to size sorting and redeposition by bottom currents. The latter hypothesis is somewhat supported by the consistent and relatively abundant occurrences of calcareous nannofossils, at least up to Sample 210-1276A-42R-CC. Fish teeth and debris also become very rare above Sample 210-1276A-41R-CC. Extensive burrowing of the sediments suggests the existence of a thriving benthic community not consistent with prolonged periods of stagnant anoxic bottom conditions.

The fine-grained autochthonous sediments typically contain rare agglutinated benthic foraminifers, black carbonized plant debris, pyrite, and occasionally rare calcareous benthic foraminifers. Rare, small specimens of calcareous benthics, including *Gyroidinoides* cf. *G. nitidus*, *Gavelinella* spp., *Praeulimina* spp., and *Bolivina* spp. occur sporadically with the agglutinated foraminifers in the mudrocks. It is likely that these bathyal and upper abyssal calcareous taxa were transported downslope turbidity currents or other gravity flows.

Lithologic Subunit 5A

Age: Cenomanian–Turonian

Interval: 210-1276A-36R-2, 129 cm, through 29R-6, 62 cm

Depth: 1129.80–1067.24 mbsf

The Cenomanian/Turonian boundary is associated with a laminated black shale interval in Sections 210-1276A-31R-2 and 31R-3, which likely correlates with OAE2. Radiolarians are generally not preserved in the sediments of lithologic Subunit 5A although they do occur commonly in two samples, once just below the OAE2 interval in Sample 210-1276A-33R-CC and once just above the event in latest Cenomanian–earliest Turonian Sample 210-1276A-31R-4, 8–12 cm. The presence of these radiolarian assemblages indicates that at the time of deposition the ocean surface waters must have oxygenated and conducive to planktonic organisms. The paucity of radiolarians recovered during the OAE2 interval corresponds to the findings of Musavu-Moussavou and Danelian (2006) in their studies of ODP Leg 207 Sites 1258 and 1261 at the Demerara Rise. These authors suggest “an intensification of euxinic conditions must have favored the proliferation of sulfate reducing bacteria, but was at the same time toxic to heterotrophic protozoa such as Radiolaria.”

Noncalcareous mudstones interpreted as in situ hemipelagic sediments in this subunit are moderately bioturbated.

The late phase of deposition of the Bonarelli level (OAE2) is likely accompanied by surface water cooling, as expressed by the calcareous nannofossil assemblage through two distinct peaks in abundance of *Eprolithus* spp. (Cores 210-1276A-31R and 29R) (Fig. F4). *Eprolithus* spp. is quite common at high latitudes and rare in the Tethyan realm. Its preference for cooler surface water might indicate cooler surface waters arriving in the Atlantic domain. This cooling event may be widespread if not a global phenomenon because *Eprolithus* peaks have been reported by several authors (Bralower, 1988; Paul et al., 1999; Nederbragt and Fiorentino, 1999; Erba, 2004) at different localities, in the Tethyan and Atlantic domain, and also in the Western Interior Basin during this time interval. Also, Sample 210-1276A-30R-3, 54–55 cm, contains the FO of the calcareous nannofossil *A. octoradiata*. This taxon seems to be highly controlled by temperature changes (Wind, 1979; Lees, 2002), being more abundant at higher latitudes, and thus, it is also a good indicator of surface water cooling. Increasing abundances of *A. octoradiata* together with *Gartnerago* spp., another taxon preferring cooler temperatures, occur in Samples 210-1276A-30R-2, 53–54 cm, and 30R-1, 49–50 cm, thus supporting an early Turonian cooling event. Global cooling is a predicted consequence of OAE2 due to the excess burial of organic matter and lowering of atmospheric pCO₂ (e.g., Arthur et al., 1988).

Lithologic Unit 4

Age: Turonian–Campanian

Interval: 210-1276A-29R-6, 62 cm, through 25R-5, 80 cm

Depth: 1067.24–1028.00 mbsf

The mineral content in the washed residues includes abundant fine-grained angular quartz, abundant mica, glauconite, pyrite, and phosphate nodules indicating dominance of terrestrial input and reworking of the sediments. The paucity of pelagic microfossils, including calcare-

ous nannofossils, and very low sedimentation rates suggest sediment starvation and shoaled CCD due to high global sea level (Thierstein, 1979; Hardenbol et al., 1998). The red oxygenated sediments indicate that the deep North Atlantic was well ventilated following a possible breach of the deepwater sill separating the North and South Atlantic ocean basins (Tucholke and Vogt, 1979).

Lithologic Unit 3

Age: Campanian–Paleocene

Interval: 210-1276A-25R-5, 80 cm, through 15R-3, 125 cm

Depth: 1028.00–929.25 mbsf

Site 1276 may have been influenced by transitional or Boreal water masses at times during the Late Cretaceous based on the presence of cool-water calcareous nannofossil taxa and the general paucity of large biserial (e.g., species of *Pseudotextularia*) and multiserial (e.g., *Planoglobulina*) planktonic foraminifers typical of Maastrichtian-age low-latitude (Tethyan) assemblages. Alternatively, dissolution during settling may have selectively removed some of these larger taxa in all but the turbiditic sandstones. A short-lived depression of the CCD (Tucholke and Vogt, 1979) or higher carbonate surface water productivity (e.g., McCarthy et al., 2004) may have provided a more favorable environment for the accumulation and preservation of planktonic foraminifers in the deep Newfoundland Basin during the latest Maastrichtian, but the richest assemblages occur in coarser-grained mudstones and very fine to fine sandstones that reflect downslope transport and size sorting.

The condensed Maastrichtian section at Site 1276 prevented the recognition of the distinct cooling/warming phases, which characterize the climatic evolution of the Maastrichtian stage (Thibault and Gardin, 2006). In particular, the *M. murus* acme, which lies within the *M. prinsii* Zone in the upper Maastrichtian, was not observed at Site 1276. This event is characterized by a strong increase of the tropical species *M. murus* coincident with a dramatic drop in abundance of “cool-water taxa,” likely indicating an extreme warming event before the end of the Mesozoic Era, (Li and Keller, 1998; Thiabault and Gardin, in press).

Regarding the K/P boundary, if only the calcareous nannofossil assemblages are considered, the boundary may be placed in Section 210-1276A-21R-4 between 41 and 49 cm (e.g., between the last Maastrichtian assemblages and the first Danian ones). However, a multiproxy analysis based on micropaleontology, magnetic susceptibility, natural gamma radiation, and $\delta^{13}\text{C}_{\text{org}}$ stable isotope analysis indicates that the boundary is more probably located at Section 210-1276A-21R-4, 55–57 cm, coincident with the first barren interval (Gardin et al., 2005, unpubl. data). If so, Sample 210-1276A-21R-4, 56–57 cm, just above the barren interval, is a witness of lowest Danian sediments (which are usually characterized by only few Cretaceous species and high thoracospherid fragments), and the overlying samples from the carbonate turbidite contain reworked Maastrichtian assemblages (Fig. F5). This succession of assemblages is comparable to that observed elsewhere at the Cretaceous–Paleogene transition, even though the abundance of Cretaceous species above the transition at Site 1276 is remarkably high, likely due to pervasive redeposition at this site. The K–P transition at Site 1276 is very peculiar because it is one of the few relatively continuous abyssal depth sections. Although there is apparent biostratigraphic

continuity, this interval is probably very condensed (reduced biozones). A small hiatus may exist across the boundary itself.

Lithologic Unit 2

Age: Paleocene–Eocene

Interval: 210-1276A-15R-3, 125 cm, through 8R-5, 113 cm

Depth: 929.25–864.73 mbsf

Relatively abundant and poorly to moderately well preserved large-size benthic foraminifers typical of warm, shallow-water carbonate platforms occur in the turbidite sandstones, together with fragments of other organisms of shallow-water origin, in the uppermost Paleocene–lower Eocene of Site 1276 (Cores 210-1276A-15R through 7R) (Georgescu et al., submitted [N2]). The large-size benthics have Caribbean affinities and are of two distinct ages. An elevated bank or banks adjacent to the Newfoundland Basin (e.g., southeast Grand Banks, southern Flemish Cap, and/or Newfoundland Seamounts) likely had tropical-subtropical communities of organisms during the Campanian–Maastrichtian and again during latest Paleocene–early Eocene time. What is especially interesting about these two ages of large-size benthics is (1) they occur in sediments corresponding with the PETM and the Early Eocene Climatic Optimum (EECO) and (2) both ages (Campanian–Maastrichtian and latest Paleocene–early Eocene) correspond with times of high sea level and global warmth (e.g., Hardenbol et al., 1998; Barerra and Savin, 1999; Zachos et al., 1993, 1994, 2001; Huber et al., 2002; Moran et al., 2006; Sluijs et al., 2006). It seems that paleobiogeographic provinces shifted farther northward during these two intervals, in part related to the existence of a proto-Gulf Stream that crossed the region of the Grand Banks (Georgescu et al., submitted [N2]).

The in situ hemipelagic deposits of lithologic Unit 2 are considered to have been deposited below the CCD at abyssal depths based on the paucity of planktonic and calcareous benthic foraminifers and the dominance of agglutinated benthic foraminifers.

Lithologic Unit 1

Age: middle Eocene–earliest Oligocene

Interval: 210-1276A-8R-5, 113 cm, through 8R-1, 50 cm

Depth: 864.73–753.00 mbsf

Nannofossil assemblages throughout this section are characterized by abundant placoliths, which are poorly preserved. This is potentially indicative of a changing hydrologic regime throughout the later Eocene–earliest Oligocene that reflects colder, more corrosive bottom currents (Wood et al., submitted [N1]). Increased bottom water circulation may be related to the onset of long-term global cooling during the middle and late Eocene (e.g., Zachos et al., 2001) or perhaps new bottom or deep water sources following the connection with the Arctic Basin (Brinkhuis et al., 2006). Furthermore, the condensed interval/potential hiatus which spans ~4.8 m.y. in the lower middle Eocene is likely the consequence of a global sea level transgression coupled with the change in hydrologic regime; this is supported by a similar condensed interval at Site 398 (Blechs Schmidt, 1979; Wood, et al., submitted [N1]).

The depositional environment of this unit is similar to lithologic Unit 2; evidence from the agglutinated foraminifer assemblages presented by Takata (2007) as well as the near-absence of planktonic foraminifers (except in redeposited sandstones) indicates deposition at abyssal depths below the CCD.

SEDIMENTATION HISTORY OF SITE 1276

The sediment accumulation rate history of Site 1276 can be divided into four broad intervals: (1) lower to middle Albian, (2) upper Albian–Cenomanian, (3) Turonian–Maastrichtian, and (4) Paleogene (Fig. F7; Table T1).

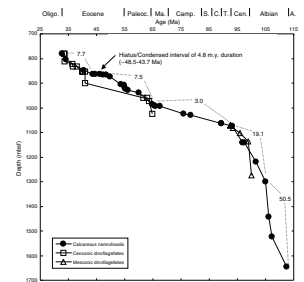
The lower to middle Albian interval had the highest average sedimentation rates (50.5 m/m.y.) of the sequence cored at Site 1276. The rates rose through the lower Albian before peaking in the middle Albian with values as high as 129 m/m.y. These high rates may be attributable to several factors, including (1) relatively low sea level and transport of clastic sediments off the shelf, (2) tectonic activity and erosion associated with the Avalon uplift on the adjacent Grand Banks (Grant et al., 1988), or (3) rapid subsidence and growing accommodation space along the toe of the slope of the Newfoundland continental margin following the onset of seafloor spreading in the Barremian (~125–129 Ma) (Tucholke, Sibuet, Klaus et al., 2004). Sedimentation rates drop to an average of 19.3 m/m.y. in the upper Albian–Cenomanian interval as sea level rose and clastics were trapped in estuaries and expanding coastal areas (Hardenbol et al., 1998).

Very low sedimentation rates and condensation characterize the Turonian–Maastrichtian interval. High global sea level and shoaling of the CCD (Thierstein, 1979; Tucholke and Vogt, 1979) likely caused the observed drop in sedimentation rates and condensation or hiatus in the lower to middle Maastrichtian. The Paleogene displays steady-state sedimentation values, although it is interrupted by a disconformity and condensed section in the lower middle Eocene that separates the Paleocene–lower Eocene and middle Eocene–basal Oligocene intervals (Fig. F6). Invigorated deepwater flow, perhaps associated with the opening of the Arctic Basin (Brinkhuis et al., 2006) or onset of global cooling following the EECO (Zachos et al., 2001), coupled with a global sea level transgression (Wood, et al., submitted [N1]), may be responsible for this disconformity and condensed section.

CONCLUSIONS

1. A nearly complete lowermost Albian (uppermost Aptian?) to lowermost Oligocene sedimentary sequence of mudrock, shale, and interbedded turbidite sandstone and other gravity flow deposits was recovered at ODP Site 1276 in the deep Newfoundland Basin. Calcareous nannofossils provide the most complete biostratigraphic age control for Site 1276. Planktonic foraminifers provide sporadic but complementary age control and are best represented in turbidite sandstones. Palynomorphs are particularly abundant and useful for biostratigraphy in organic-rich Paleogene and mid-Cretaceous sediments.
2. Site 1276 has been at abyssal depths (>2000 m) near or below the CCD since earliest Albian time (~112 Ma). Calcareous microfossils

F7. Age-depth plot, p. 47.



sils are not abundant, except in some turbidites. In situ mudrock and shale are characterized by abyssal agglutinated foraminifers and varying quantities of radiolarians, phosphatic fish debris, sponge spicules, and plant debris. Calcareous nannofossils are generally present in many samples owing to their transport to the deep sea in fecal pellets or distal turbidites.

3. The Albian part of the succession accumulated very rapidly in response to erosion on the Grand Banks associated with the Avalon uplift, increased sedimentation associated with relatively low sea level, and/or increased accommodation space associated with subsidence of the young Newfoundland continental margin.
4. Two mid-Cretaceous OAEs are well developed at Site 1276. Basal Albian OAE1b occurs in Cores 210-1276A-95R and 94R, and Cenomanian/Turonian boundary OAE2 occurs in Sections 210-1276A-31R-2 and 3. Both OAEs lack benthic biota in the laminated black shale, suggesting that anoxia may have existed through much of the basal water column, thereby contrasting the expanded oxygen minimum zone model for OAE development.
5. Calcareous nannofossil assemblages suggest surface water cooling in the vicinity of Site 1276 following OAE2 in the early Turonian. This may be a widespread if not global phenomenon related to the excess burial of carbon during OAE2.
6. Much of the Upper Cretaceous (Turonian–Maastrichtian) is represented by a relatively condensed sequence of oxidized sediments due to the combined influences of high global sea level, elevated CCD, and invigorated deepwater circulation during the Late Cretaceous.
7. A biostratigraphically complete Cretaceous/Paleogene boundary was recovered in Section 210-1276A-21R-4. This represents one of the deepest water K/P boundary sections known.
8. The discovery of redeposited large-size benthic foraminifers with Caribbean affinities in Cores 210-1276A-15R through 7R demonstrate that a shallow-water carbonate platform(s) existed nearby on the southeastern Grand Banks, Newfoundland Seamounts, or southern Flemish Cap during the Campanian–Maastrichtian and again during the latest Paleocene and early Eocene. Both time intervals correspond with high sea level and global warmth. These findings suggest that paleobiogeographic boundaries shifted much further north and that a proto-Gulf Stream probably crossed the offshore Newfoundland region at these times.
9. A probable hiatus and condensed interval spanning ~4.8 m.y. in the early middle Eocene (~48.5–43.7 Ma) suggest that invigorated bottom water flow and a change in global eustatic sea level accompanied the onset of global cooling, or opening of the Arctic Basin, following the early Eocene Climatic Optimum (EECO).

ACKNOWLEDGMENTS

This research used samples and/or data provided by the Ocean Drilling Program (ODP). ODP is sponsored by the U.S. National Science Foundation and participating countries under management of Joint Oceanographic Institutions (JOI), Inc. R.M.L. would like to acknowledge postcruise science support from the U.S. Science Support Panel. E.U. thanks JOI for support to sail on ODP Leg 210 and to attend the second postcruise meeting. J.P. acknowledges support through the Ger-

man Research Foundation (DFG). We thank Denise Kulhanek, Felix Gradstein, and an anonymous reviewer for their thoughtful and helpful input. We would also like to thank all of our Leg 210 shipmates and crew for ensuring such a scientifically successful and enjoyable final ODP expedition.

REFERENCES

- Angori, E., and Monechi, S., 1996. High-resolution calcareous nannofossil biostratigraphy across the Paleocene/Eocene boundary at Caravaca (southern Spain). *Israel J. Earth Sci.*, 44:197–206.
- Applegate, J.L., and Bergen, J.A., 1988. Cretaceous calcareous nannofossil biostratigraphy of sediments recovered from the Galicia margin, ODP Leg 103. In Boillot, G., Winterer, E.L., et al., *Proc. ODP, Sci. Results*, 103: College Station, TX (Ocean Drilling Program), 293–348. doi:10.2973/odp.proc.sr.103.144.1988
- Arthur, M.A., Dean, W.E., and Pratt, L.M., 1988. Geochemical and climatic effects of increased marine organic carbon burial at the Cenomanian/Turonian boundary. *Nature (London, U. K.)*, 335(6192):714–717. doi:10.1038/335714a0
- Barrera, E., and Savin, S.M., 1999. Evolution of Campanian–Maastrichtian marine climates and oceans. In Barrera, E., and Johnson, C.C. (Eds.), *Evolution of the Cretaceous Ocean–Climate System*. Spec. Pap.—Geol. Soc. Am., 332:245–282.
- Bellier, J.-P., Moullade, M., and Huber, B.T., 2000. Mid-Cretaceous planktonic foraminifers from Blake Nose: revised biostratigraphic framework. In Kroon, D., Norris, R.D., and Klaus, A. (Eds.), *Proc. ODP, Sci. Results*, 171B: College Station, TX (Ocean Drilling Program), 1–12. doi:10.2973/odp.proc.sr.171B.111.2000
- Berggren, W.A., Kent, D.V., Swisher, C.C., III, and Aubry, M.-P., 1995. A revised Cenozoic geochronology and chronostratigraphy. In Berggren, W.A., Kent, D.V., Aubry, M.-P., and Hardenbol, J. (Eds.), *Geochronology, Time Scales and Global Stratigraphic Correlation*. Spec. Publ.—SEPM (Soc. Sediment. Geol.), 54:129–212.
- Blebschmidt, G., 1979. Biostratigraphy of calcareous nannofossils: Leg 47B, Deep Sea Drilling Project. In Sibuet, J.C., Ryan, W.B.F., et al., *Init. Repts. DSDP*, 47 (Pt. 2): Washington, DC (U.S. Govt. Printing Office), 327–360. doi:10.2973/dsdp.proc.47-2.106.1979
- Bralower, T.J., 1988. Calcareous nannofossil biostratigraphy and assemblages of the Cenomanian/Turonian boundary interval: implications for the origin and timing of oceanic anoxia. *Paleoceanography*, 8:275–316.
- Bralower, T.J., 2002. Evidence of surface water oligotrophy during the late Paleocene–Eocene Thermal Maximum: nannofossil assemblage data from Ocean Drilling Program Site 690, Maud Rise, Weddell Sea. *Paleoceanography*, 17(2):1–12. doi:10.1029/2001PA000662
- Bralower, T.J., and Bergen, J.A., 1998. Cenomanian–Santonian calcareous nannofossil biostratigraphy of a transect of cores drilled across the western interior seaway. In Arthur, M.A., and Dean, W.E. (Eds.), *Stratigraphy and Paleoenvironments of the Cretaceous Western Interior Seaway*. SEPM Concepts Sedimentol. Paleontol., 6:59–77.
- Bralower, T.J., Leckie, R.M., Sliter, W.V., and Thierstein, H.R., 1995a. An integrated Cretaceous microfossil biostratigraphy. In Berggren, W.A., Kent, D.V., Aubry, M.-P., and Hardenbol, J. (Eds.), *Geochronology, Time Scales, and Global Stratigraphic Correlation*. Spec. Publ.—SEPM (Soc. Sediment. Geol.), 54:65–79.
- Bralower, T.J., Sliter, W.V., Arthur, M.A., Leckie, R.M., Allard, D.J., and Schlanger, S.O., 1993. Dysoxic/anoxic episodes in the Aptian–Albian (Early Cretaceous). In Pringle, M.S., Sager, W.W., Sliter, W.V., and Stein, S. (Eds.), *The Mesozoic Pacific: Geology, Tectonics, and Volcanism*. Geophys. Monogr., 77:5–37.
- Bralower, T.J., Zachos, J.C., Thomas, E., Parrow, M., Paull, C.K., Kelly, D.C., Premoli Silva, I., Sliter, W.V., and Lohmann, K.C., 1995b. Late Paleocene to Eocene paleoceanography of the equatorial Pacific Ocean: stable isotopes recorded at Ocean Drilling Program Site 865, Allison Guyot. *Paleoceanography*, 10(4):841–865. doi:10.1029/95PA01143
- Bréhéret, J.G., 1994. The mid-Cretaceous organic-rich sediments from the Vocontian zone of the French Southeast Basin. In Mascle, A. (Ed.), *Hydrocarbon and Petroleum Geology of France*: New York (Springer Verlag), 295–320.

- Brinkhuis, H., Schouten, S., Collinson, M.E., Sluijs, A., Sinninghe Damsté, J.S., Dickens, G.R., Huber, M., Cronin, T.M., Onodera, J., Takahashi, K., Bujak, J.P., Stein, R., van der Burgh, J., Eldrett, J.S., Harding, I.C., Lotter, A.F., Sangiorgi, F., van Konijnenburg-van Cittert, H., de Leeuw, J.W., Matthiessen, J., Backman, J., Moran, K., and the Expedition 302 Scientists, 2006. Episodic fresh surface waters in the Eocene Arctic Ocean. *Nature (London, U. K.)*, 441(7093):606–609. doi:10.1038/nature04692
- Bukry, D., 1973. Low-latitude coccolith biostratigraphic zonation. In Edgar, N.T., Saunders, J.B., et al., *Init. Repts. DSDP*, 15: Washington (U.S. Govt. Printing Office), 685–703. doi:10.2973/dsdp.proc.15.116.1973
- Bukry, D., 1975. Coccolith and silicoflagellate stratigraphy, northwestern Pacific Ocean, Deep Sea Drilling Project Leg 32. In Larson, R.L., Moberly, R., et al., *Init. Repts. DSDP*, 32: Washington (U.S. Govt. Printing Office), 677–701. doi:10.2973/dsdp.proc.32.124.1975
- Burnett, J.A., Gallagher, L.T., and Hampton, M.J., 1998. Upper Cretaceous. In Bown, P.R. (Ed.), *Calcareous Nannofossil Biostratigraphy*: Dordrecht, The Netherlands (Kluwer Academic Publ.), 132–199.
- Caron, M., 1985. Cretaceous planktic foraminifera. In Bolli, H.M., Saunders, J.B., and Perch-Nielsen, K. (Eds.), *Plankton Stratigraphy*: Cambridge (Cambridge Univ. Press), 17–86.
- Coccioni, R., Erba, E., and Premoli-Silva, I., 1992. Barremian–Aptian calcareous plankton biostratigraphy from the Gorgo Cerbara section (Marche, central Italy) and implications for plankton evolution. *Cretaceous Res.*, 13(5–6):517–537. doi:10.1016/0195-6671(92)90015-I
- Coccioni, R., and Galeotti, S., 2003. The mid-Cenomanian event: prelude to OAE 2. *Palaeogeogr., Palaeoclimatol., Palaeoecol.*, 190:427–440. doi:10.1016/S0031-0182(02)00617-X
- Erba, E., 2004. Calcareous nannofossils and Mesozoic oceanic anoxic events. *Mar. Micropaleontol.*, 52(1–4):85–106. doi:10.1016/j.marmicro.2004.04.007
- Erba, E., Castradori, D., Guasti, G., and Ripepe, M., 1992. Calcareous nannofossils and Milankovitch cycles: the example of the Albian gault clay formation (southern England). *Palaeogeogr., Palaeoclimatol., Palaeoecol.*, 93(1–2):47–69. doi:10.1016/0031-0182(92)90183-6
- Erbacher, J., Gerth, W., Schmiedl, G., and Hemleben, C., 1998. Benthic foraminiferal assemblages of late Aptian–early Albian black shale intervals in the Vocontian Basin, SE France. *Cretaceous Res.*, 19(6):805–826. doi:10.1006/cres.1998.0134
- Erbacher, J., Hemleben, C., Huber, B., and Markey, M., 1999. Correlating environmental changes during early Albian Oceanic Anoxic Event 1B using benthic foraminiferal paleoecology. *Mar. Micropaleontol.*, 38(1):7–28. doi:10.1016/S0377-8398(99)00036-5
- Erbacher, J., Huber, B.T., Norris, R.D., and Markey, M., 2001. Intensified thermohaline stratification as a possible cause for an ocean anoxic event in the Cretaceous period. *Nature (London, U. K.)*, 409(6818):325–327. doi:10.1038/35053041
- Erbacher, J., Thurow, J., and Littke, R., 1996. Evolution patterns of radiolaria and organic matter variations: a new approach to identify sea-level changes in mid-Cretaceous pelagic environments. *Geology*, 24:499–502. doi:10.1130/0091-7613(1996)024<0499:EPORAO>2.3.CO;2
- Galbrun, B., and Gardin, S., 2004. New chronostratigraphy of the Cretaceous–Paleogene boundary interval at Bidart (France). *Earth Planet. Sci. Lett.*, 224(1–2):19–32. doi:10.1016/j.epsl.2004.04.043
- Gardin, S., Galbrun, B., Leckie, M., Pearce, C., Wilson, C., and Ladner, B., 2005. The abyssal record of the K-P boundary at Site 1276A, Leg 210 (Newfoundland Basin): results from a multidisciplinary approach. In Godet, A., Mort, H., and Boden, S. (Eds.), *7th Int. Symp. Cretaceous: Sci. Program Abstr.*, 89–90.

- Gardin, S., and Monechi, S., 1998. Paleoeological change in middle to low-latitude calcareous nannoplankton at the Cretaceous/Tertiary boundary. *Bull. Soc. Geol. Fr.*, 169:709–723.
- Gartner, S., 1996. Calcareous nannofossils at the Cretaceous–Tertiary boundary. In MacLeod, N., and Keller, G. (Eds.), *Cretaceous–Tertiary Mass Extinctions: Biotic and Environmental Changes*: London (Norton), 27–47.
- Grant, A.C., Jansa, L.F., McAlpine, K.D., and Edwards, A., 1988. Mesozoic–Cenozoic geology of the eastern margin of the Grand Banks and its relation to Galicia Bank. In Boillot, G., Winterer, E.L., et al., *Proc. ODP, Sci. Results*, 103: College Station, TX (Ocean Drilling Program), 787–808. doi:10.2973/odp.proc.sr.103.173.1988
- Hardenbol, J., Thierry, J., Farley, M.B., de Graciansky, P.-C., and Vail, P.R., 1998. Mesozoic and Cenozoic sequence chronostratigraphic framework of European basins. In de Graciansky, P.-C., Hardenbol, J., Jacquin, T., and Vail, P.R. (Eds.), *Mesozoic and Cenozoic Sequence Stratigraphy of European Basins*. Spec. Publ.—SEPM (Soc. Sediment. Geol.), 60:3–13.
- Honjo, S., 1975. Dissolution of suspended coccoliths in the deep-sea water column and sedimentation of coccolith ooze. In Sliter, W.V., Bé, A.W.H., and Berger, W.H. (Eds.), *Dissolution of Deep-Sea Carbonates*. Spec. Publ.—Cushman Found. Foraminiferal Res., 13:115–128.
- Honjo, S., 1976. Coccoliths: production, transportation and sedimentation. *Mar. Micropaleontol.*, 1:65–79. doi:10.1016/0377-8398(76)90005-0
- Huber, B.T., Norris, R.D., and MacLeod, K.G., 2002. Deep sea paleotemperature record of extreme warmth during the Cretaceous. *Geology*, 30(2):123–126. doi:10.1130/0091-7613(2002)030<0123:DSPROE>2.0.CO;2
- Jiang, M.J., and Gartner, S., 1986. Calcareous nannofossil succession across the Cretaceous/Tertiary boundary in east-central Texas. *Micropaleontology*, 32(3):232–255. doi:10.2307/1485619
- Kaminski, M.A., Kuhnt, W., and Moullade, M., 1999. The evolution and paleobiogeography of abyssal agglutinated foraminifera since the Early Cretaceous: a tale of four faunas. *Neues Jahrb. Geol. Palaeontol., Abh.*, 212(1–3):401–439.
- Kelly, D.C., Bralower, T.J., Zachos, J.C., Premoli Silva, I., and Thomas, E., 1996. Rapid diversification of planktonic foraminifera in the tropical Pacific (ODP Site 865) during the Late Paleocene Thermal Maximum. *Geology*, 24(5):423–426. doi:10.1130/0091-7613(1996)024<0423:RDOPFI>2.3.CO;2
- Kennedy, W.J., Gale, A.S., Bown, P.R., Caron, M., Davey, R.J., Gröcke, D., and Wray, D.S., 2000. Integrated stratigraphy across the Aptian–Albian boundary in the Marnes Bleues, at the Col de Pré-Guittard, Arnayon (Drôme), and at Tartonne (Alpes-de-Haute-Provence), France: a candidate global boundary stratotype section and boundary point for the base of the Albian stage. *Cretaceous Res.*, 21(5):591–720. doi:10.1006/cres.2000.0223
- Kuhnt, W., and Urquhart, E., 2001. Tethyan flysch-type benthic foraminiferal assemblages in the North Atlantic: Cretaceous to Paleogene deep water agglutinated foraminifera from the Iberia Abyssal Plain (ODP Leg 173). *Rev. Micropaleontol.*, 44(1):27–58. doi:10.1016/S0035-1598(01)90074-1
- Kuypers, M.M.M., Blokker, P., Erbacher, J., Kinkel, H., Pancost, R.D., Schouten, S., and Sinninghe Damsté, J.S., 2001. Massive expansion of marine archaea during a mid-Cretaceous oceanic anoxic event. *Science*, 293(5527):92–94. doi:10.1126/science.1058424
- Leckie, R.M., 1984. Mid-Cretaceous planktonic foraminiferal biostratigraphy off central Morocco, DSDP Leg 79, Sites 545 and 547. In Hinz, K., Winterer, E.L., et al., *Init. Repts. DSDP*, 79: Washington (U.S. Govt. Printing Office), 579–620. doi:10.2973/dsdp.proc.79.122.1984
- Leckie, R.M., Bralower, T.J., and Cashman, R., 2002. Oceanic anoxic events and plankton evolution: biotic response to tectonic forcing during the mid-Cretaceous. *Paleoceanography*, 17(3):1041. doi:10.1029/2001PA000623

- Lees, J.A., 2002. Calcareous nannofossil biogeography illustrates palaeoclimate change in the Late Cretaceous Indian Ocean. *Cretaceous Res.*, 23:537–634. doi:10.1006/cres.2003.1021
- Li, L., and Keller, G., 1998. Abrupt deep-sea warming at the end of the Cretaceous. *Geology*, 26(11):995–998. doi:10.1130/0091-7613(1998)026<0995:ADSWAT>2.3.CO;2
- Luciani, V., and Cobianchi, M., 1999. The Bonarelli level and other black shales in the Cenomanian–Turonian of the northeastern dolomites (Italy): calcareous nannofossil and foraminiferal data. *Cretaceous Res.*, 20(2):135–167. doi:10.1006/cres.1999.0146
- Martini, E., 1971. Standard Tertiary and Quaternary calcareous nannoplankton zonation. In Farinacci, A. (Ed.), *Proc. 2nd Int. Conf. Planktonic Microfossils Roma*: Rome (Ed. Tecnosci.), 2:739–785.
- McCarthy, F.M.G., Findlay, D.J., and Little, M.L., 2004. The micropaleontological character of anomalous calcareous sediments of late Pliocene through early Pleistocene age below the CCD in the northwestern North Pacific Ocean. *Palaeogeogr., Palaeoclimatol., Palaeoecol.*, 215(1–2):1–15. doi:10.1016/j.palaeo.2004.07.032
- McGonigal, K.L., and Wise, S.W., Jr., 2001. Eocene calcareous nannofossil biostratigraphy and sediment accumulation of turbidite sequences on the Iberia Abyssal Plain, ODP Sites 1067–1069. In Beslier, M.-O., Whitmarsh, R.B., Wallace, P.J., and Girardeau, J. (Eds.), *Proc. ODP, Sci. Results*, 173: College Station, TX (Ocean Drilling Program), 1–35. doi:10.2973/odp.proc.sr.173.008.2001
- Monechi, S., Angori, E., and von Salis, K., 2000. Calcareous nannofossil turnover around the Paleocene/Eocene transition at Alamedilla (southern Spain). *Bull. Soc. Geol. Fr.*, 171:477–489.
- Moran, K., Backman, J., Brinkhuis, H., Clemens, S.C., Cronin, T., Dickens, G.R., Eynaud, F., Gattacceca, J., Jakobsson, M., Jordan, R.W., Makinski, M., King, J., Koc, N., Krylov, A., Martinez, N., Matthiessen, J., McInroy, D., Moore, T.C., Onodera, J., O'Regan, M., Pälike, H., Rea, B., Rio, D., Sakamoto, T., Smith, D.C., Stein, R., St. John, K., Suto, I., Suzuki, N., Takahashi, K., Watanabe, M., Yamamoto, M., Farrell, J., Frank, M., Kubik, P., Jokat, W., and Kristoffersen, Y., 2006. The Cenozoic palaeoenvironment of the Arctic Ocean. *Nature (London, U. K.)*, 441(7093):601–605. doi:10.1038/nature04800
- Musavu-Moussavou, B., and Danelian, T., 2006. The radiolarian biotic response to Oceanic Anoxic Event 2 in the southern part of the northern proto-Atlantic (Demerara Rise, ODP Leg 207). *Rev. Micropaleontol.*, 49(3):141–163. doi:10.1016/j.revmic.2006.04.004
- Nederbragt, A.J., and Fiorentino, A., 1999. Stratigraphy and palaeoceanography of the Cenomanian–Turonian boundary event in Oued Mellegue, north-western Tunisia. *Cretaceous Res.*, 20(1):47–62. doi:10.1006/cres.1998.0136
- Okada, H., and Bukry, D., 1980. Supplementary modification and introduction of code numbers to the low-latitude coccolith biostratigraphic zonation (Bukry, 1973; 1975). *Mar. Micropaleontol.*, 5:321–325. doi:10.1016/0377-8398(80)90016-X
- Paul, C.R.C., Lamolda, M.A., Mitchell, S.F., Vaziri, M.R., Gorostidi, A., and Marshall, J.D., 1999. The Cenomanian–Turonian boundary at Eastbourne (Sussex, UK): a proposed European reference section. *Palaeogeogr., Palaeoclimatol., Palaeoecol.*, 150(1–2):83–121. doi:10.1016/S0031-0182(99)00009-7
- Perch-Nielsen, K., 1979. Calcareous nannofossils from the Cretaceous between the North Sea and the Mediterranean. In Wiedmann, J. (Ed.), *Aspekte der Kreide Europas*. Int. Union Geol. Sci. Ser. A, 6:223–272.
- Perch-Nielsen, K., 1985. Mesozoic calcareous nannofossils. In Bolli, H.M., Saunders, J.B., and Perch-Nielsen, K. (Eds.), *Plankton Stratigraphy*: Cambridge (Cambridge Univ. Press), 329–426.
- Pilskaln, C.H., and Honjo, S., 1987. The fecal pellet fraction of biogeochemical particle fluxes to the deep sea. *Global Biogeochem. Cycles*, 1:31–48.

- Premoli Silva, I., Erba, E., and Tornaghi, M.E., 1989. Palaeoenvironmental signals and changes in surface water fertility in mid-Cretaceous corg-rich pelagic facies of the Fucoid marls (central Italy). *Geobios. Mem. Spec.*, 11:225–236.
- Premoli Silva, I., and Sliter, W.V., 1994. Cretaceous planktonic foraminiferal biostratigraphy and evolutionary trends from the Bottaccione section, Gubbio, Italy. *Palaeontogr. Ital.*, 82:2–90.
- Premoli Silva, I., and Sliter, W.V., 1999. Cretaceous paleoceanography: evidence from planktonic foraminiferal evolution. In Barrera, E., and Johnson, C.C. (Eds.), *The Evolution of Cretaceous Ocean-Climatic System*. Spec. Pap.—Geol. Soc. Am., 332:301–328.
- Raffi, I., Backman, J., and Pälke, H., 2005. Changes in calcareous nannofossil assemblages across the Paleocene/Eocene transition from the paleo-equatorial Pacific Ocean. *Palaeogeogr., Palaeoclimatol., Palaeoecol.*, 226(1–2):93–126. doi:10.1016/j.palaeo.2005.05.006
- Röhl, U., Bralower, T.J., Norris, R.D., and Wefer, G., 2000. New chronology for the Late Paleocene Thermal Maximum and its environmental implications. *Geology*, 28(10):927–930. doi:10.1130/0091-7613(2000)028<0927:NCFTLP>2.3.CO;2
- Roth, P.H., 1973. Calcareous nannofossils—Leg 17, Deep Sea Drilling Project. In Winterer, E.L., Ewing, J.I., et al., *Init. Repts. DSDP*, 17: Washington (U.S. Govt. Printing Office), 695–795. doi:10.2973/dsdp.proc.17.123.1973
- Roth, P.H., 1983. Jurassic and Lower Cretaceous calcareous nannofossils in the western North Atlantic (Site 534): biostratigraphy, preservation, and some observations on biogeography and paleoceanography. In Sheridan, R.E., Gradstein, F.M., et al., *Init. Repts. DSDP*, 76: Washington (U.S. Govt. Printing Office), 587–621. doi:10.2973/dsdp.proc.76.125.1983
- Roth, P.H., and Bowdler, J., 1981. Middle Cretaceous calcareous nannoplankton biogeography and oceanography of the Atlantic Ocean. In Warme, J.E., Douglas, R.G., and Winterer, E.L. (Eds.), *The Deep Sea Drilling Project: a Decade of Progress*. Spec. Publ.—Soc. Econ. Paleontol. Mineral., 32:517–546.
- Shipboard Scientific Party, 2004. Explanatory notes. In Tucholke, B.E., Sibuet, J.-C., Klaus, A., et al., *Proc. ODP, Init. Repts.*, 210: College Station, TX (Ocean Drilling Program), 1–69. doi:10.2973/odp.proc.ir.210.102.2004
- Sissingh, W., 1977. Biostratigraphy of Cretaceous calcareous nannoplankton. *Geol. Mijnbouw*, 56:37–65.
- Sluijs, A., Schouten, S., Pagani, M., Woltering, M., Brinkhuis, H., Sinninghe Damsté, J.S., Dickens, G.R., Huber, M., Reichert, G.-J., Stein, R., Matthiessen, J., Lourens, L.J., Pedentchouk, N., Backman, J., Moran, K., and the Expedition 302 Scientists, 2006. Subtropical Arctic Ocean temperatures during the Palaeocene/Eocene Thermal Maximum. *Nature (London, U. K.)*, 441(7093):610–613. doi:10.1038/nature04668
- Sliter, W.V., 1989. Biostratigraphic zonation for Cretaceous planktonic foraminifers examined in thin section. *J. Foraminiferal Res.*, 19:1–19.
- Steinmetz, J.C., 1994. Stable isotopes in modern coccolithophores. In Winter, A., and Siesser, W. (Eds.), *Coccolithophores*: Cambridge (Cambridge Univ. Press).
- Thibault, N., and Gardin, S., 2006. Maastrichtian calcareous nannofossil biostratigraphy and paleoecology in the equatorial Atlantic (Demerara Rise, ODP Leg 207 Hole 1258A). In Erbacher, J., Danelian, T., and Nishi, H. (Eds.), *Demerara Rise (Leg 207): Equatorial Cretaceous and Palaeogene Stratigraphy and Paleoceanography, Part II*. Rev. Micropaleontol., 49(4):199–214. doi:10.1016/j.revmic.2006.08.002
- Thibault, N., and Gardin, S., in press. The late Maastrichtian nannofossil record of climate change in the South Atlantic DSDP Hole 525A. *Mar. Micropaleontol.*
- Thierstein, H.R., 1979. Paleoceanographic implications of organic carbon and carbonate distribution in Mesozoic deep sea sediments. In Talwani, M., Hay, W., and Ryan, W.B.F. (Eds.), *Deep Drilling Results in the Atlantic Ocean*. Maurice Ewing Ser., 3:249–274.
- Thomas, E., and Shackleton, N., 1996. The Palaeocene–Eocene benthic foraminiferal extinction and stable isotope anomalies. In Knox, R.W.O'B., Corfield, R.M., and

- Dunay, R.E. (Eds.), *Correlation of the Early Paleogene in Northwest Europe*. Geol. Soc. Spec. Publ., 101:401–441.
- Thurrow, J., 1988. Cretaceous radiolarians of the North Atlantic Ocean: ODP Leg 103 (Sites 638, 640, and 641) and DSDP Legs 93 (Site 603) and 47B (Site 398). In Boillot, G., Winterer, E.L., et al., *Proc. ODP, Sci. Results*, 103: College Station, TX (Ocean Drilling Program), 379–418. [doi:10.2973/odp.proc.sr.103.148.1988](https://doi.org/10.2973/odp.proc.sr.103.148.1988)
- Tremolada, F., and Bralower, T.J., 2004. Nannofossil assemblage fluctuations during the Paleocene–Eocene Thermal Maximum at Sites 213 (Indian Ocean) and 401 (North Atlantic Ocean): paleoceanographic implications. *Mar. Micropaleontol.*, 52(1–4):107–116. [doi:10.1016/j.marmicro.2004.04.002](https://doi.org/10.1016/j.marmicro.2004.04.002)
- Tucholke, B.E., Sibuet, J.-C., Klaus, A., et al., 2004. *Proc. ODP, Init. Repts.*, 210: College Station, TX (Ocean Drilling Program). [doi:10.2973/odp.proc.ir.210.2004](https://doi.org/10.2973/odp.proc.ir.210.2004)
- Tucholke, B.E., and Vogt, P.R., 1979. Western North Atlantic: sedimentary evolution and aspects of tectonic history. In Tucholke, B.E., Vogt, P.R., et al., *Init. Repts. DSDP*, 43: Washington (U.S. Govt. Printing Office), 791–825. [doi:10.2973/dsdp.proc.43.140.1979](https://doi.org/10.2973/dsdp.proc.43.140.1979)
- Van Heck, S.E., and Prins, B., 1987. A refined nannoplankton zonation for the Danian of the central North Sea. *Abh. Geol. Bundesanst. (Austria)*, 39:285–303.
- Varol, O., 1989. Palaeocene calcareous nannofossil biostratigraphy. In Crux, J.A., and van Heck, S.E. (Eds.), *Nannofossils and Their Applications*: Chichester (Ellis Horwood), 267–310.
- Watkins, D.K., Bralower, T.J., Covington, J.M., and Fisher, C.G., 1993. Biostratigraphy and paleoecology of the Upper Cretaceous calcareous nannofossils in the Western Interior Basin, North America. In Cauldwell, W.G.E., and Kauffmann, E.G. (Eds.), *Evolution of the Western Interior Basin*. Geol. Assoc. Can. Spec. Pap., 39:521–538.
- Wind, F.H., 1979. Maestrichtian–Campanian nannofloral provinces of the southern Atlantic and Indian Oceans. In Talwani, M., Hay, W., and Ryan, W.B.F. (Eds.), *Deep Sea Drilling Results in the Atlantic Ocean: Continental Margins and Paleoenvironment*. Maurice Ewing Ser., 3:123–137.
- Zachos, J.C., Lohmann, K.C., Walker, J.C.G., and Wise, S.W., Jr., 1993. Abrupt climate changes and transient climates during the Paleogene: a marine perspective. *J. Geol.*, 101:191–213.
- Zachos, J.C., Pagani, M., Sloan, L., Thomas, E., and Billups, K., 2001. Trends, rhythms, and aberrations in global climate 65 Ma to present. *Science*, 292(5517):686–693. [doi:10.1126/science.1059412](https://doi.org/10.1126/science.1059412)
- Zachos, J.C., Stott, L.D., and Lohmann, K.C., 1994. Evolution of early Cenozoic marine temperatures. *Paleoceanography*, 9(2):353–387. [doi:10.1029/93PA03266](https://doi.org/10.1029/93PA03266)

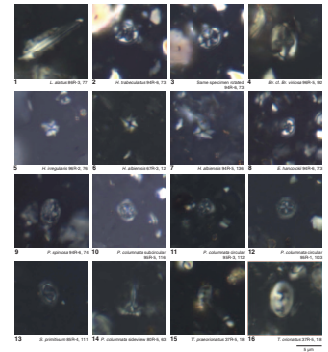
APPENDIX

Taxonomic list of calcareous nannofossils taxa cited in text

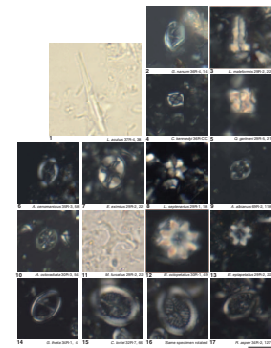
Representative species are illustrated in Plates P1, P2, P3, and P4.

Ahmuellerella octoradiata (Gorka, 1957) Reinhardt (1966)
Arkhangelskiella cymbiformis Vekshina (1959)
Axopodorhabdus albianus (Black, 1967) Wind and Wise in Wise and Wind (1977)
Biantholithus sparsus Bramlette and Martini (1964)
Biscutum constans (Gorka, 1957) Black in Black and Barnes (1959)
Blackites rectus Deflandre in Deflandre and Fert (1954)
Blackites spinosus (Deflandre and Fert, 1954) Hay and Towe (1962)
Braarudosphaera batilliformis Troelsen and Quadros (1971)
Braarudosphaera bigelowii (Gran and Braarud, 1935) Deflandre (1947)
Calcidiscus Kamptner (1950)
Chiasmolithus altus Bukry and Percival (1971)
Chiasmolithus bidens (Bramlette and Sullivan, 1961), Hay and Mohler (1967)
Chiasmolithus consuetus (Bramlette and Sullivan, 1961), Hay and Mohler (1967)
Chiasmolithus expansus (Bramlette and Sullivan) Gartner (1970)
Chiasmolithus gigas (Bramlette and Sullivan, 1961) Radomski (1968)
Chiasmolithus grandis (Bramlette and Riedel) Radomski (1968)
Chiasmolithus oamaruensis (Deflandre, 1954) Hay, Mohler, and Wade (1966)
Chiasmolithus solitus (Bramlette and Sullivan) Locker (1968)
Clausicoccus subdistichus (Roth and Hay, 1967) Prins (1979)
Coccolithus formosus (Kamptner) Wise (1973)
Coccolithus pelagicus (Wallich) Schiller (1930)
Corollithion kennedyi Crux (1981)
Cretarhabdus loriei Gartner (1968)
Cribrosphaerella daniae Perch-Nielsen (1983)
Cruciplacolithus asymmetricus Van Heck and Prins (1987)
Cruciplacolithus cruciformis (Hay and Towe, 1962) Roth (1970)
Cruciplacolithus edwardsii Romein (1979)
Cruciplacolithus intermedius Van Heck and Prins (1987)
Cruciplacolithus primus Perch-Nielsen (1977)
Cyclagelosphaera reinhardtii (Perch-Nielsen, 1968) Romein (1977)
Cyclicargolithus floridanus (Hay et al., 1967) Bukry (1971)
Cyclicargolithus obrutus (Perch-Nielsen, 1971) Prins (1979)
Cylindralithus nudus Bukry (1969)
Discoaster anartios Bybell (1998)
Discoaster araneus Bukry (1971)
Discoaster barbadiensis (Tan, 1927) Bramlette and Riedel (1954)
Discoaster binodosus Martini (1958)
Discoaster deflandrei Bramlette and Riedel (1954)
Discoaster diastypus Bramlette and Sullivan (1961)
Discoaster lodoensis Bramlette and Riedel (1954)
Discoaster mahmoudii Perch-Nielsen (1981)
Discoaster multiradiatus Bramlette and Riedel (1954)
Discoaster nobilis Martini (1961)
Discoaster saipanensis Bramlette and Riedel (1954)
Discoaster salisburgensis Stradner (1961)
Discoaster sublodoensis Bramlette and Sullivan (1961)
Discoaster tani nodifer Bramlette and Riedel (1954)
Discorhabdus rotatorius (Bukry, 1969) Thierstein (1974)
Eprolithus eptapetalus Varol (1991)
Eprolithus octopetalus Varol (1991)
Eiffellithus eximius (Stover, 1966) Perch-Nielsen (1968)
Eiffellithus monechiae Crux (1991)
Eiffellithus turriseiffelii (Deflandre in Deflandre and Fert, 1954) Reinhardt (1965)

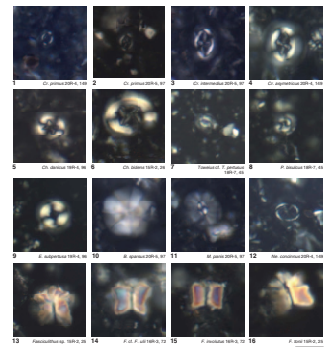
P1. Albian, p. 49.



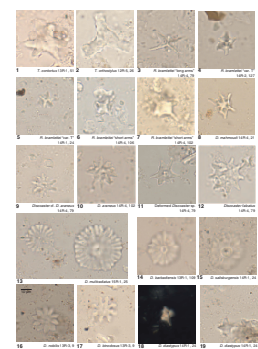
P2. Cenomanian–Turonian, p. 50.



P3. Danian, p. 51.



P4. Paleocene–Eocene, p. 52.



Eiffellithus? hancockii Burnett (1998)
Ellipsolithus macellus (Bramlette and Sullivan, 1961) Sullivan (1964)
Ericsonia robusta Hay and Mohler (1967)
Ericsonia subpertusa Hay and Mohler (1967)
Fasciculithus alanii Perch-Nielsen (1971)
Fasciculithus bitectus Romein (1979)
Fasciculithus magnicordis (1979)
Fasciculithus magnus Bukry and Percival (1971)
Fasciculithus schaubii Hay and Mohler (1967)
Fasciculithus thomasii Perch-Nielsen (1971)
Fasciculithus tonii Perch-Nielsen (1971)
Fasciculithus tympaniformis Hay and Mohler in Hay et al. (1967)
Fasciculithus ulii Perch-Nielsen (1971)
Gartnerago nanum Thierstein (1974)
Gartnerago theta (Black in Black and Barnes, 1959) Jakubowski (1986)
Hayesites albiensis Manivit (1971)
Hayesites irregularis (Thierstein in Roth and Thierstein, 1972) Applegate et al. in Covington and Wise (1987)
Helenea chiasia Worsley 1971
Helicosphaera euphratis Haq (1966)
Heliolithus cantabriae Perch-Nielsen (1971)
Heliolithus kleinpellii Sullivan (1964)
Heliolithus riedelii Bramlette and Sullivan (1961)
Kamptnerius magnificus Deflandre (1959)
Lanternithus minutus Stradner (1962)
Lithastrinus septenarius Forchaimer (1972)
Lithraphidites acutus Verbeek and Manivit in Manivit et al. (1977)
Lithraphidites alatus Thierstein in Roth and Thierstein (1972)
Lithraphidites quadratus Bramlette and Martini (1964) emend. Roth (1978)
Markalius inversus (Deflandre in Deflandre and Fert, 1954) Bramlette and Martini (1964)
Markalius panis (Edwards) Jiang and Gartner (1986)
Marthasterites furcatus (Deflandre in Deflandre and Fert, 1954) Deflandre (1959)
Micula decussata Vekshina (1959)
Micula murus (Martini, 1961) Bukry (1973)
Micula prinsii Perch-Nielsen (1979)
Nannotetrina cristata (Martini, 1958) Perch-Nielsen (1971)
Nannotetrina quadrata (Bramlette and Sullivan, 1961) Bukry (1973)
Nannotetrina Achuthan and Stradner (1969)
Neobiscutum parvulum (Romein, 1979) Varol (1989)
Neobiscutum romeinii (Perch-Nielsen, 1981) Varol (1989)
Neochiastozygus modestus Perch-Nielsen (1971)
Neochiastozygus perfectus Perch-Nielsen (1971)
Neococcolithes dubius (Deflandre, 1954) Black (1967)
Neorepidolithus Romein (1979)
Nephrolithus frequens Gorke (1957)
Pemma basquensis (Martini, 1959) Báldi-Beke (1971)
Pemma papillatum Martini (1959)
Pontosphaera multipora (Kamptner, 1948) Roth (1970)
Pontosphaera spp. Lohmann (1902)
Prediscosphaera columnata (Stover, 1966) Perch-Nielsen (1984)
Prediscosphaera cretacea (Arkhangelsky, 1912) Gartner (1968)
Prediscosphaera spinosa Bramlette and Martini (1964) Gartner (1968)
Prediscosphaera stoveri (Perch-Nielsen, 1968) Shafik and Stradner (1971)
Prinsius dimorphosus (Perch-Nielsen, 1969) Perch-Nielsen (1977)
Prinsius martinii (Perch-Nielsen, 1969) Haq (1971)
Prinsius tenuiculum (Okada and Thierstein, 1979) Perch-Nielsen (1984)
Psyktosphaera firthii Pospichal and Wise (1990)
Quadrum gartneri Prins and Perch-Nielsen in Manivit et al. (1977)
Quadrum intermedium Varol (1992)
Reinhardtites anthophorus (Deflandre, 1959) Perch-Nielsen, 1968

Reinhardtites levis Prins and Sissingh in Sissingh, 1977
Reticulofenestra bisecta (Hay, Mohler, and Wade, 1966) Roth (1970)
Reticulofenestra dictyoda (Deflandre in Deflandre and Fert, 1954) Stradner in Stradner and Edwards (1968)
Reticulofenestra hillae Bukry and Percival (1971)
Reticulofenestra oamaruensis (Deflandre in Deflandre and Fert, 1954) Stradner in Haq (1968)
Reticulofenestra reticulata (Gartner and Smith, 1967) Roth and Thierstein (1972)
Reticulofenestra samodurovii (Hay, Mohler, and Wade, 1966) Roth (1970)
Reticulofenestra scrippsae (Bukry and Percival, 1971) Roth (1973)
Reticulofenestra Hay, Mohler, and Wade (1966)
Reticulofenestra umbilica (Levin, 1965) Martini and Ritzkowski (1968)
Rhabdosphaera inflata Bramlette and Sullivan (1961)
Rhabdosphaera perlonga (Deflandre in Grassé, 1952) Bramlette and Sullivan (1961)
Rhabdosphaera Haeckel (1894)
Rhomboaster bramlettei (Bronnimann and Stradner, 1960) Bybell and Self Trail (1995)
Rhomboaster spineus (Shafik and Stradner, 1971) Perch-Nielsen (1984)
Scyphosphaera spp. Lohmann (1902)
Sphenolithus anarrhopus Bukry and Bramlette (1969)
Sphenolithus editus Perch-Nielsen in Perch-Nielsen et al. (1978)
Sphenolithus primus Perch-Nielsen (1971)
Sphenolithus moriformis (Bronnimann and Stradner, 1960) Bramlette and Wilcoxson (1967)
Sphenolithus radians Deflandre in Grassé (1952)
Sphenolithus Deflandre in Grassé (1952)
Sullivania danica (Brotzen, 1959) Varol (1992)
Thoracosphaera Schiller (1930)
Toweius Hay and Mohler (1967)
Tranolithus orionatus (Reinhardt, 1966) Reinhardt (1966)
Tranolithus praeorionatus Bown in Kennedy et al. (2004)
Transversopontis pulcheroides (Sullivan, 1964) Baldi-Beke (1971)
Tribrachiatus contortus (Stradner, 1958) Bukry (1982)
Tribrachiatus orthostylus Shamrai (1963)
Uniplanarius sissinghi Perch-Nielsen 1986b
Uniplanarius trifidus (Stradner in Stradner and Papp, 1961) Hattner and Wise (1980)
Watznaueria barnesiae (Black, 1959) Perch-Nielsen (1968)
Zeugrhabdotus erectus (Deflandre in Deflandre and Fert, 1954) Reinhardt (1965)
Zeugrhabdotus moulladei Bergen (1994)
Zeugrhabdotus sigmoides Bramlette and Sullivan (1961)
Zygrhablithus bijugatus (Deflandre in Deflandre and Fert, 1954) Deflandre (1959).

Figure F1. Bathymetry of the Newfoundland margin showing the locations of Sites 1276 and 1277. Bathymetric contour interval = 100 m. Smts. = seamounts.

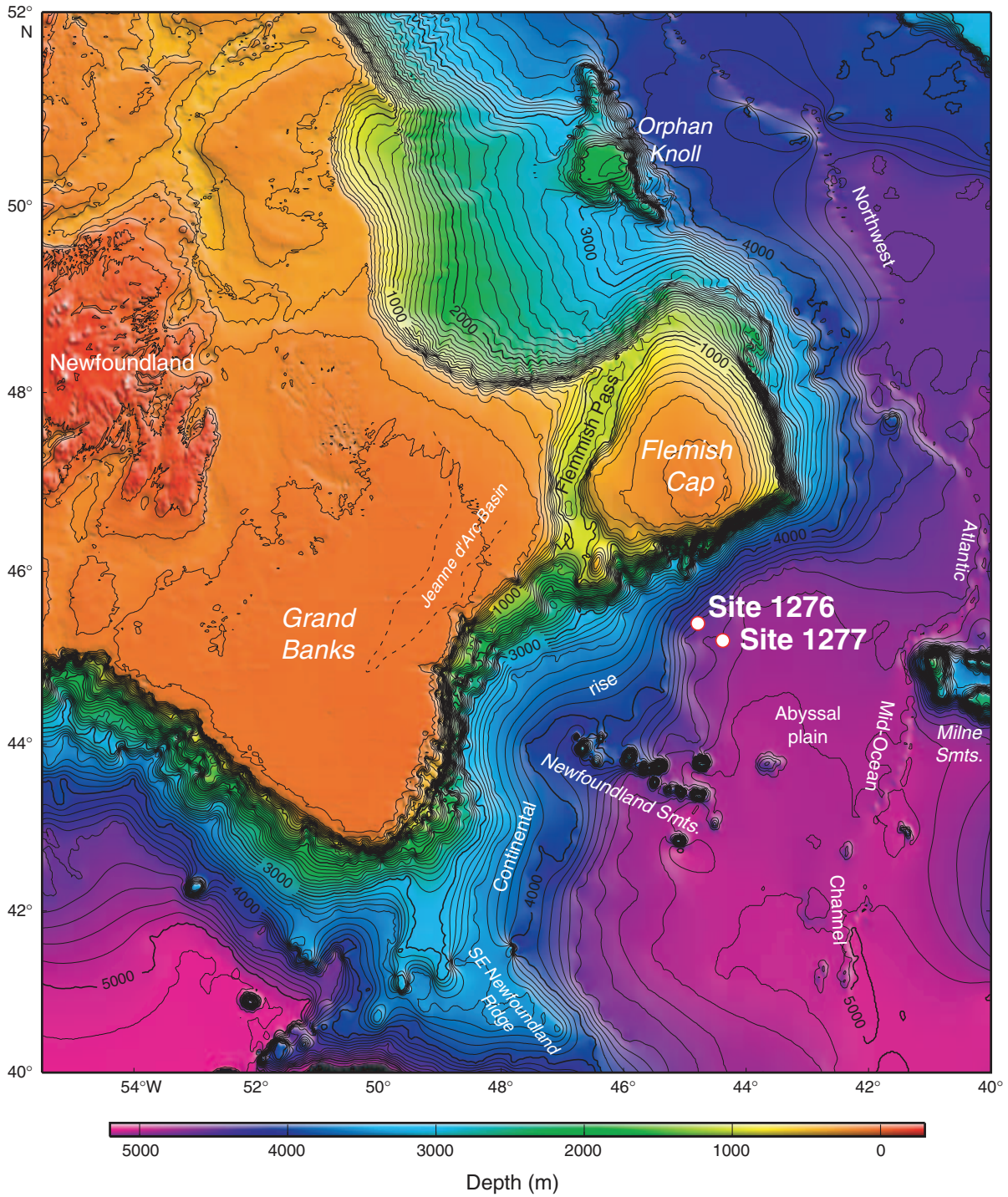


Figure F2. Calcareous nannofossil and planktonic foraminiferal zonal schemes (see “Materials and Methods,” p. 3, and Shipboard Scientific Party [2004], for details). T = top, B = bottom, BA = bottom acme. (Continued on next three pages.)

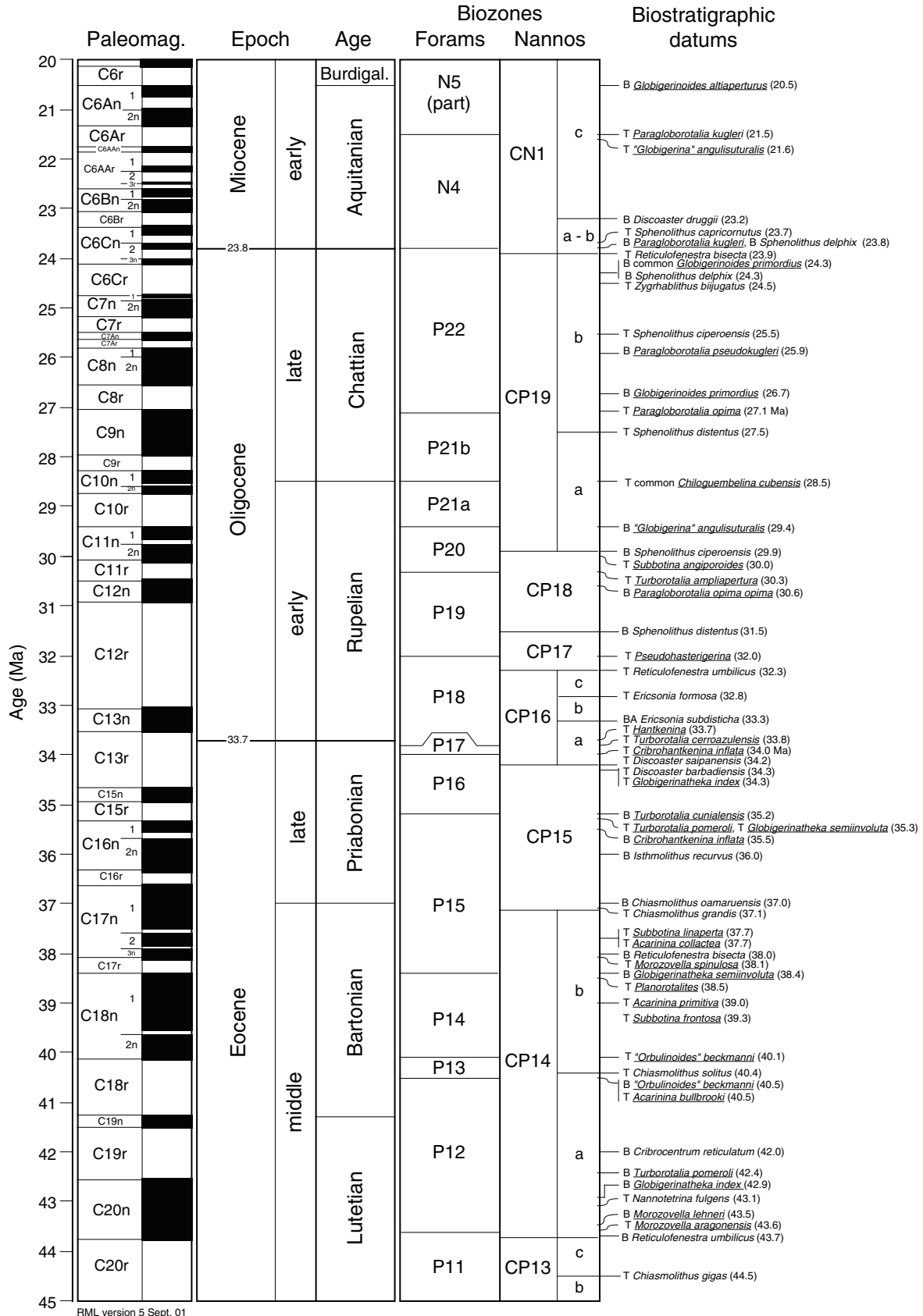


Figure F2 (continued).

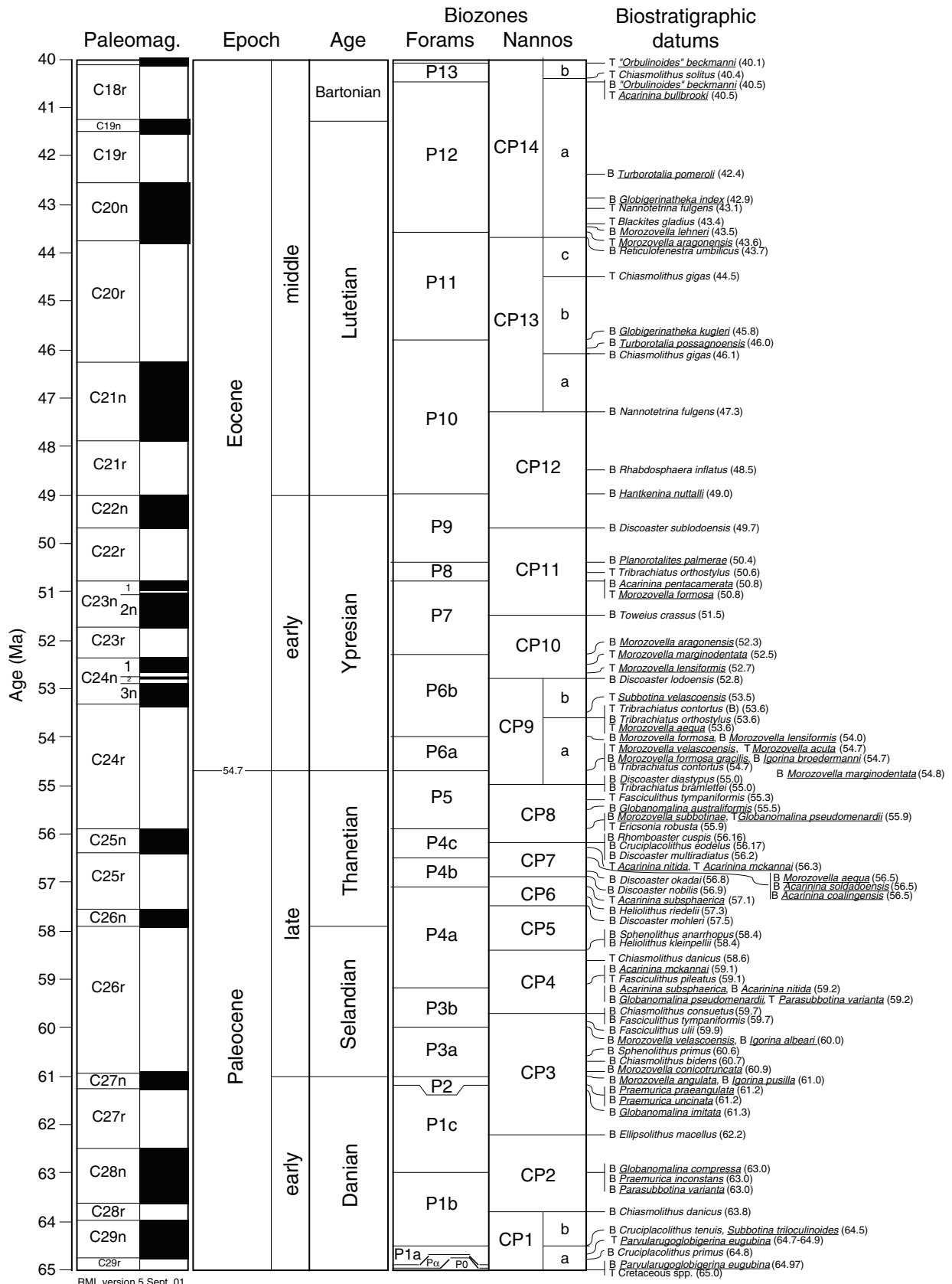


Figure F2 (continued).

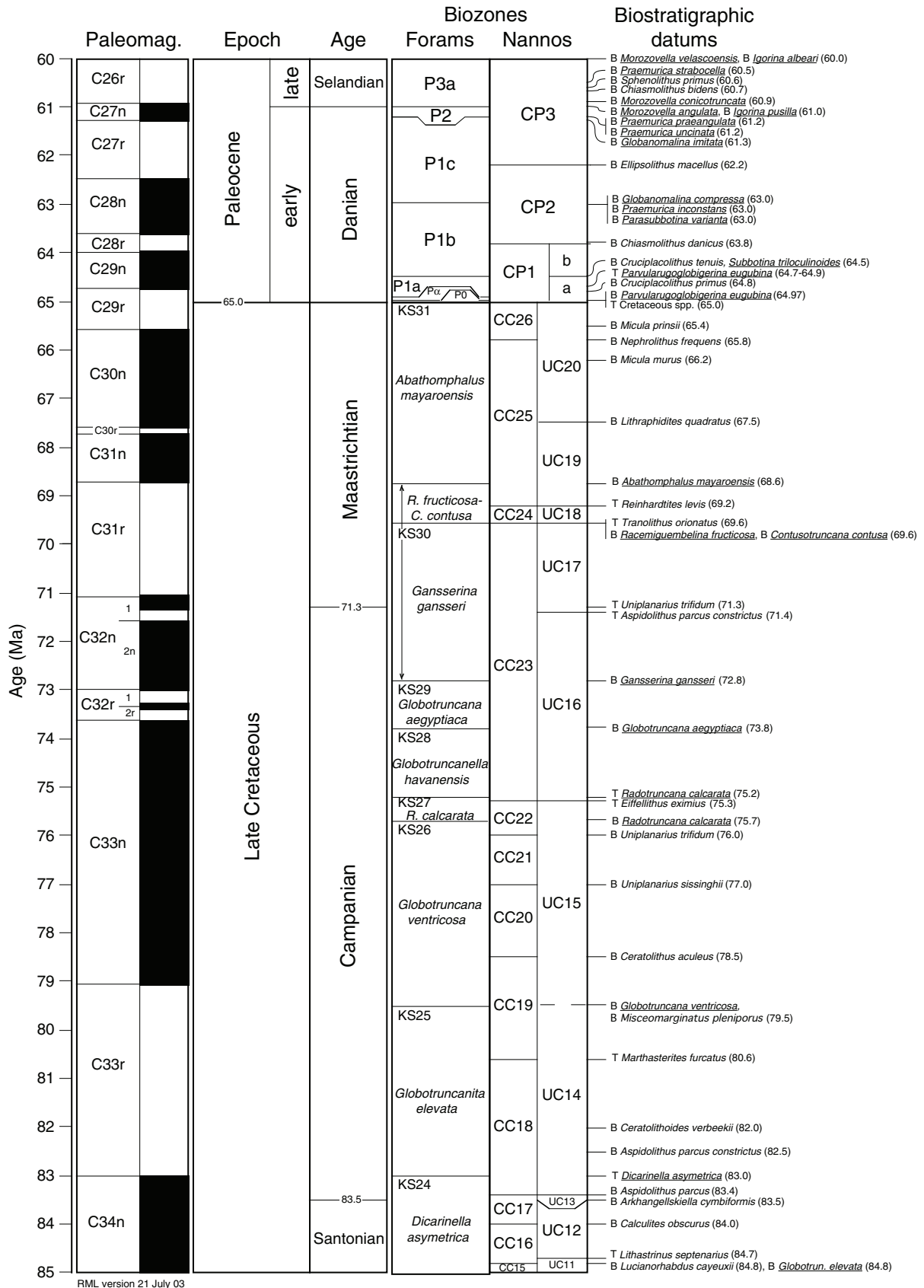


Figure F2 (continued).

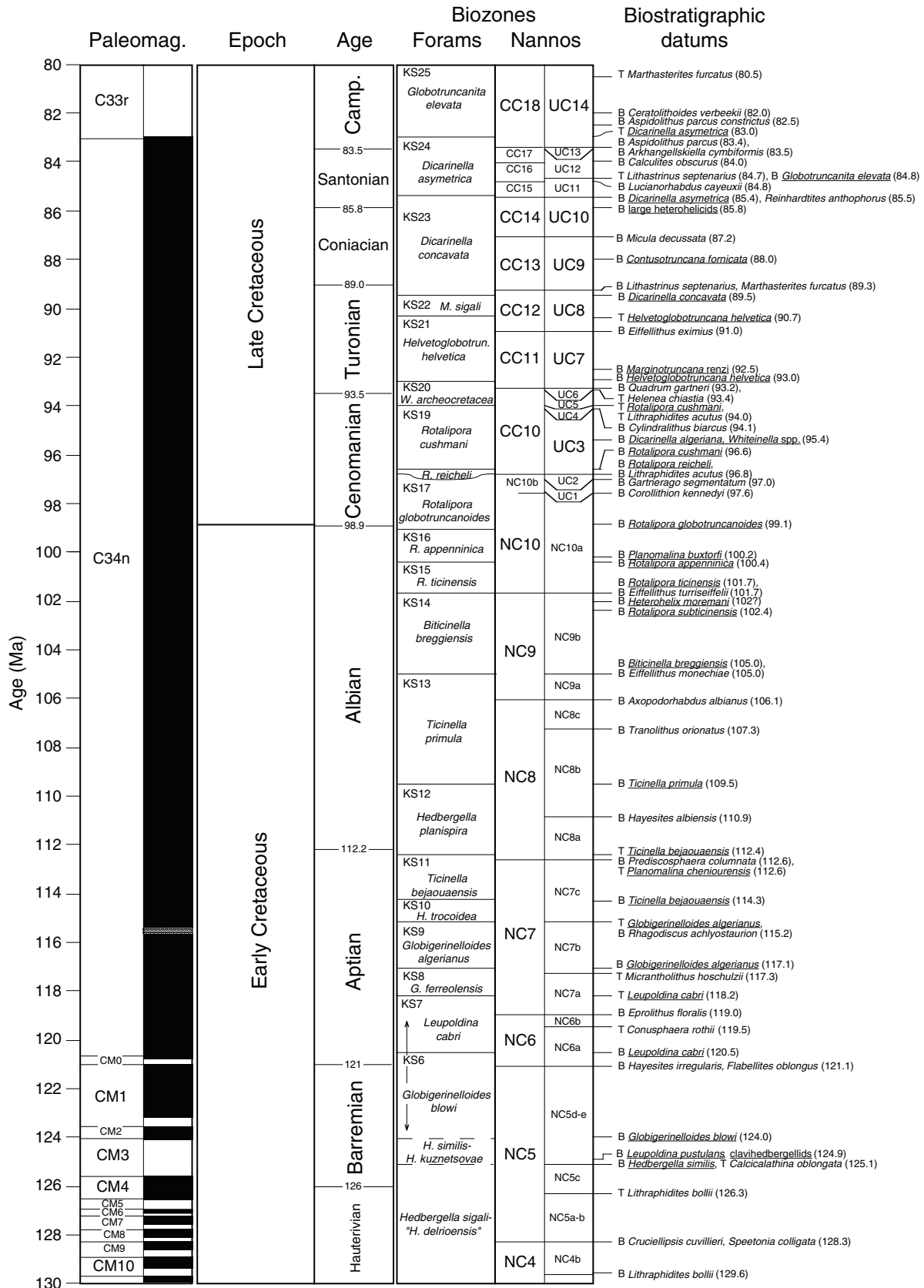


Figure F3. Microfossil biostratigraphy compared to depth, lithology, and core recovery. (Continued on next two pages.)

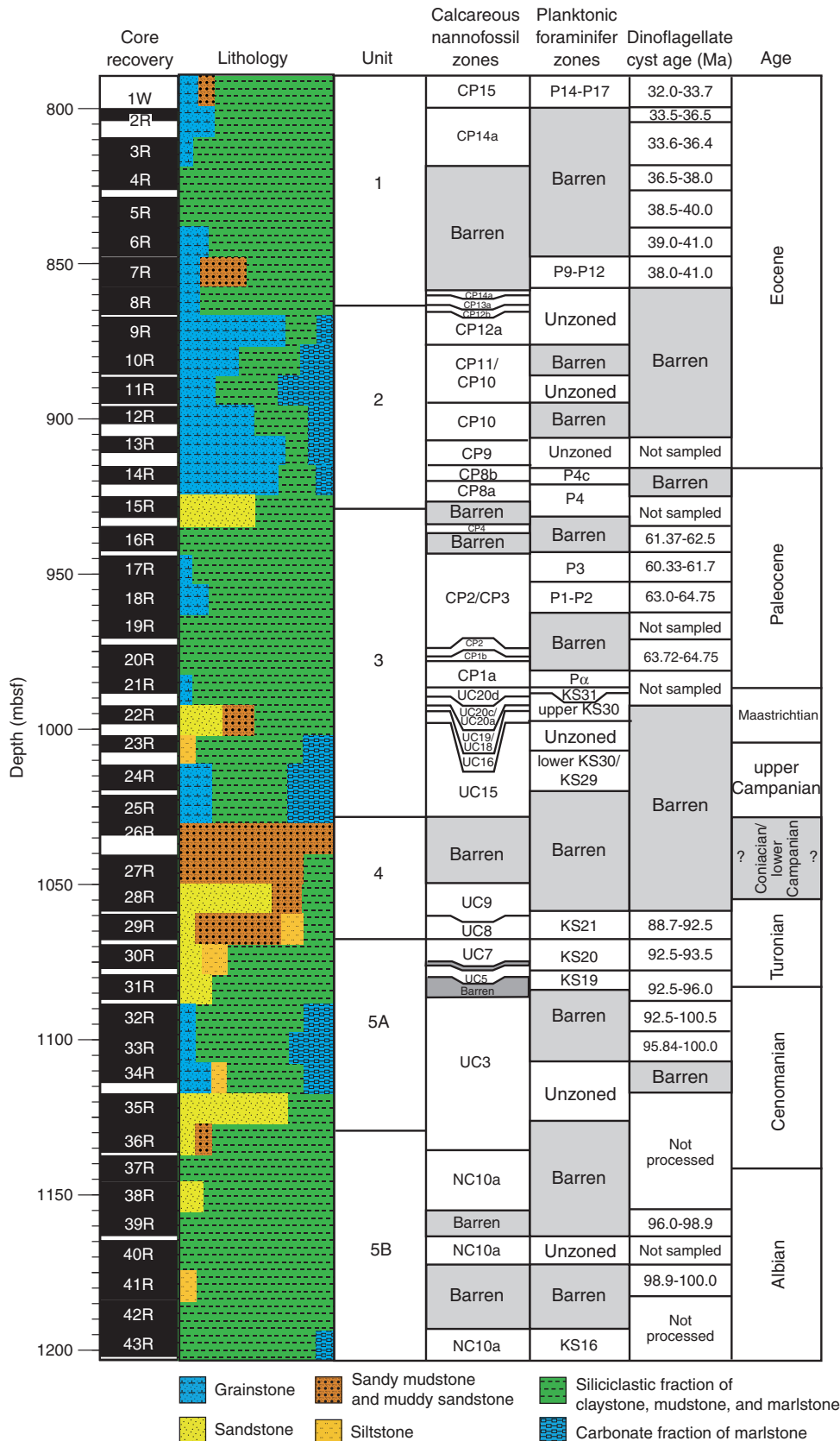


Figure F3 (continued).

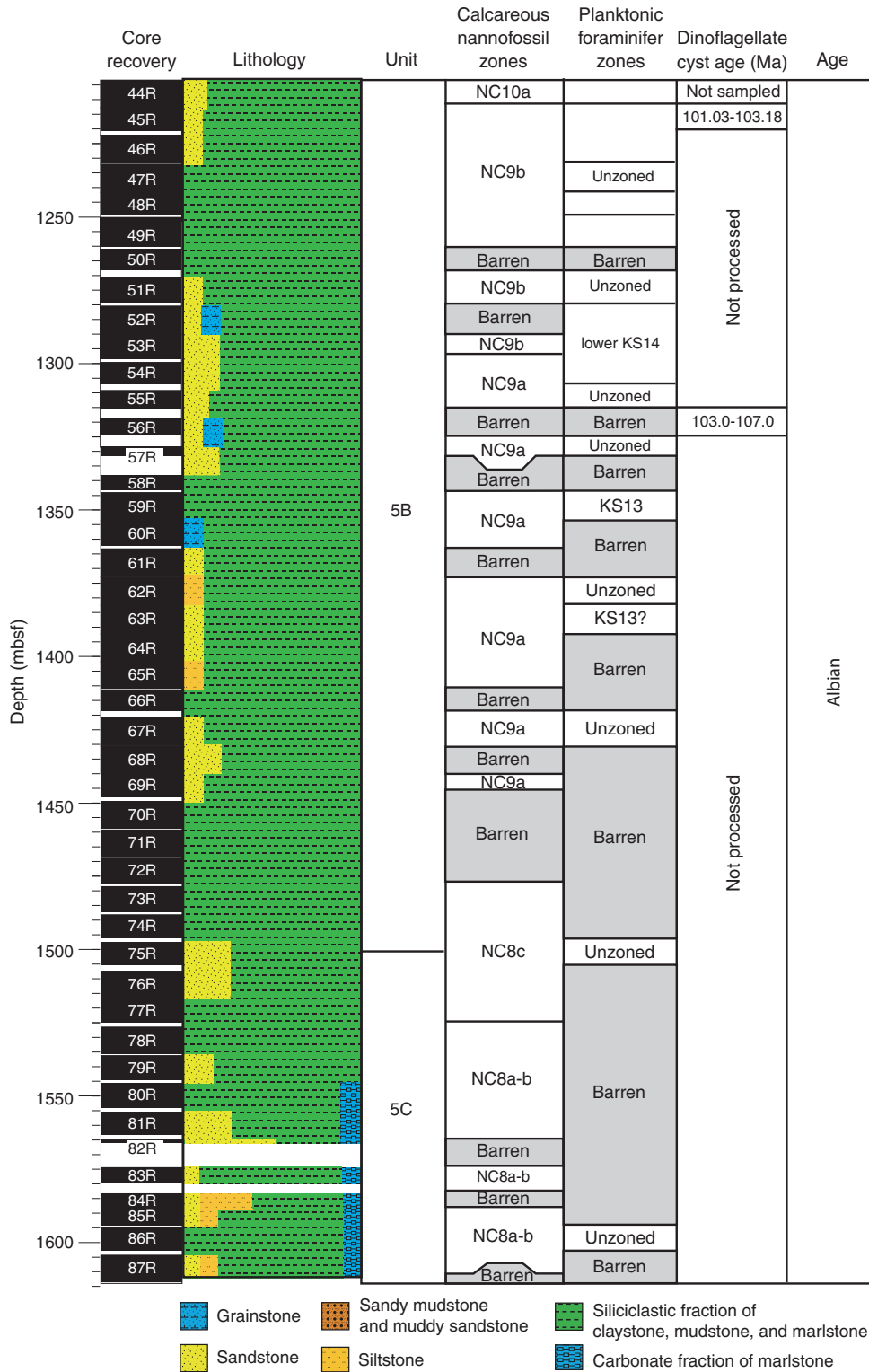


Figure F3 (continued).

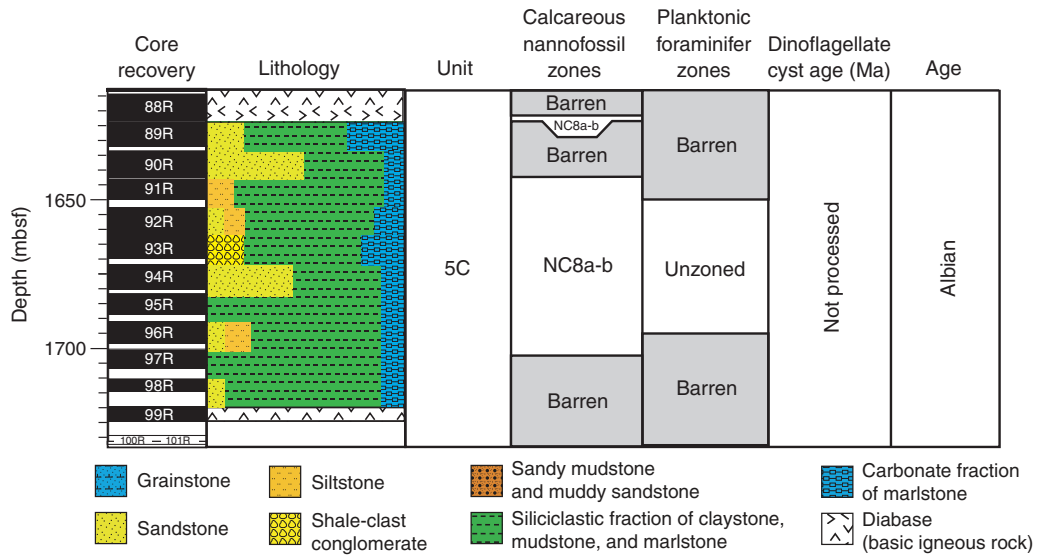


Figure F4. Cenomanian–Turonian calcareous nannofossil bioevents at Site 1276.

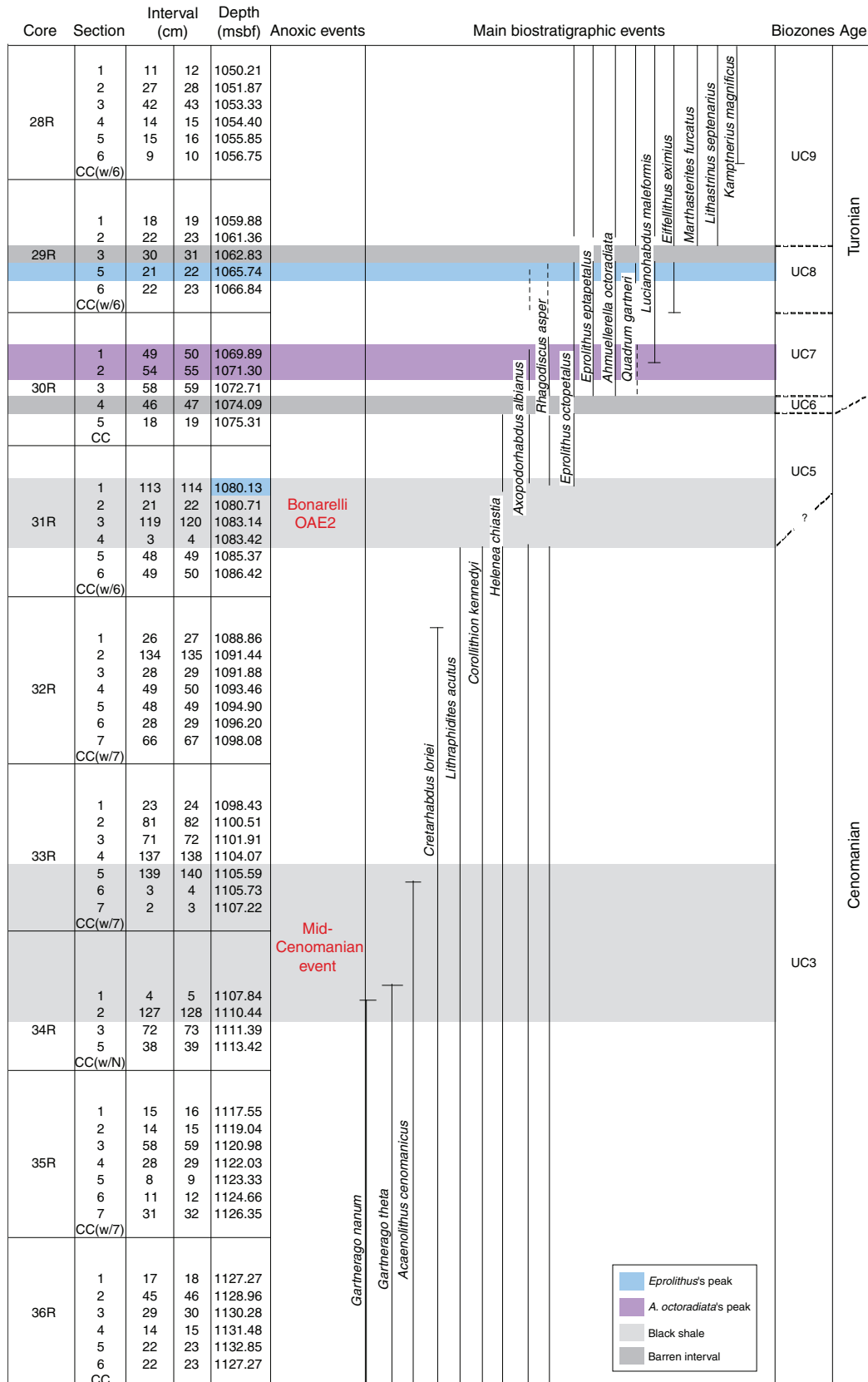


Figure F5. Mid-Campanian to early Paleogene calcareous nannofossil bioevents at Site 1276.

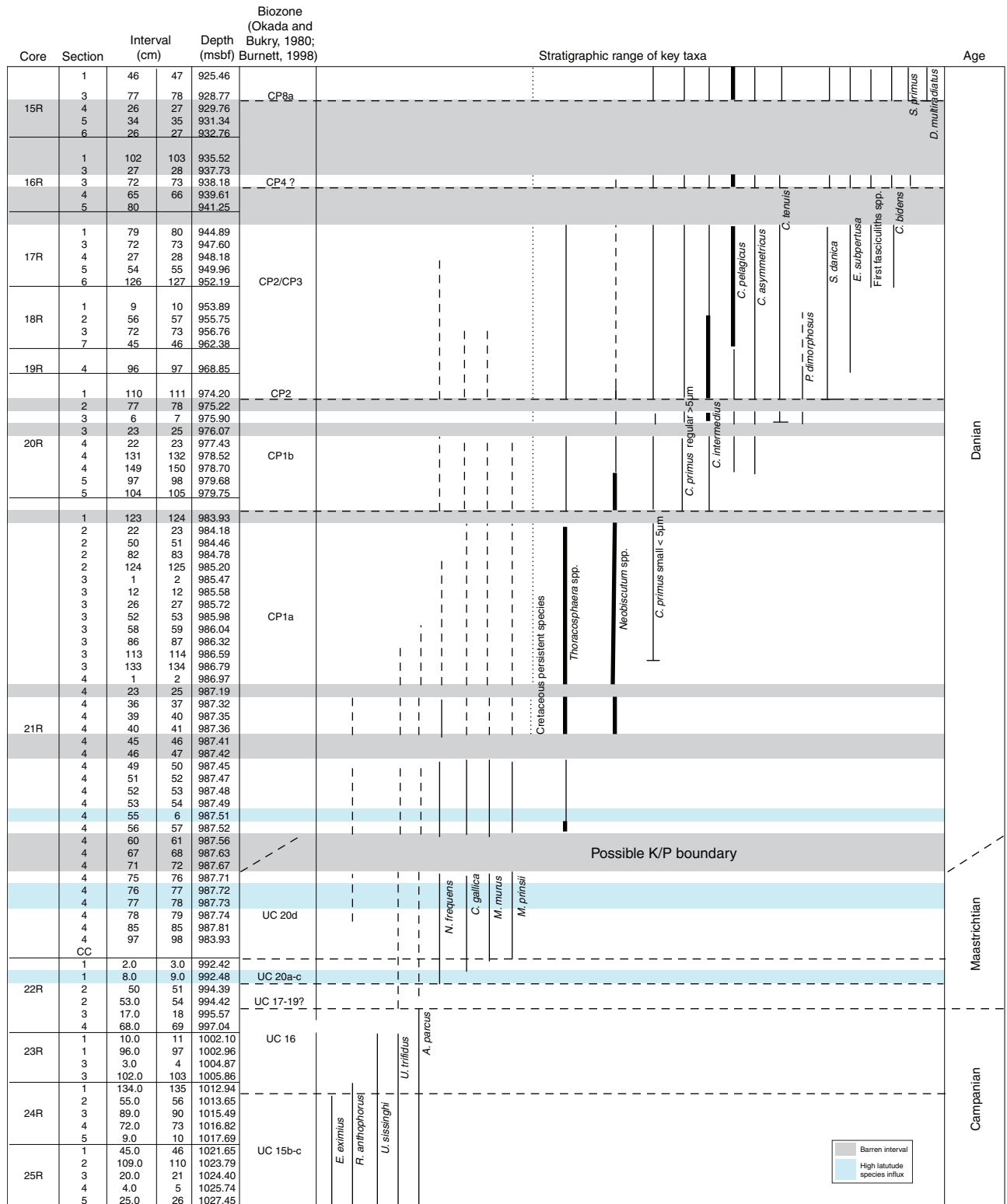


Figure F6. Calcareous nannofossil bioevents across the Paleocene–Eocene transition at Site 1276. Shaded area = inferred PETM interval.

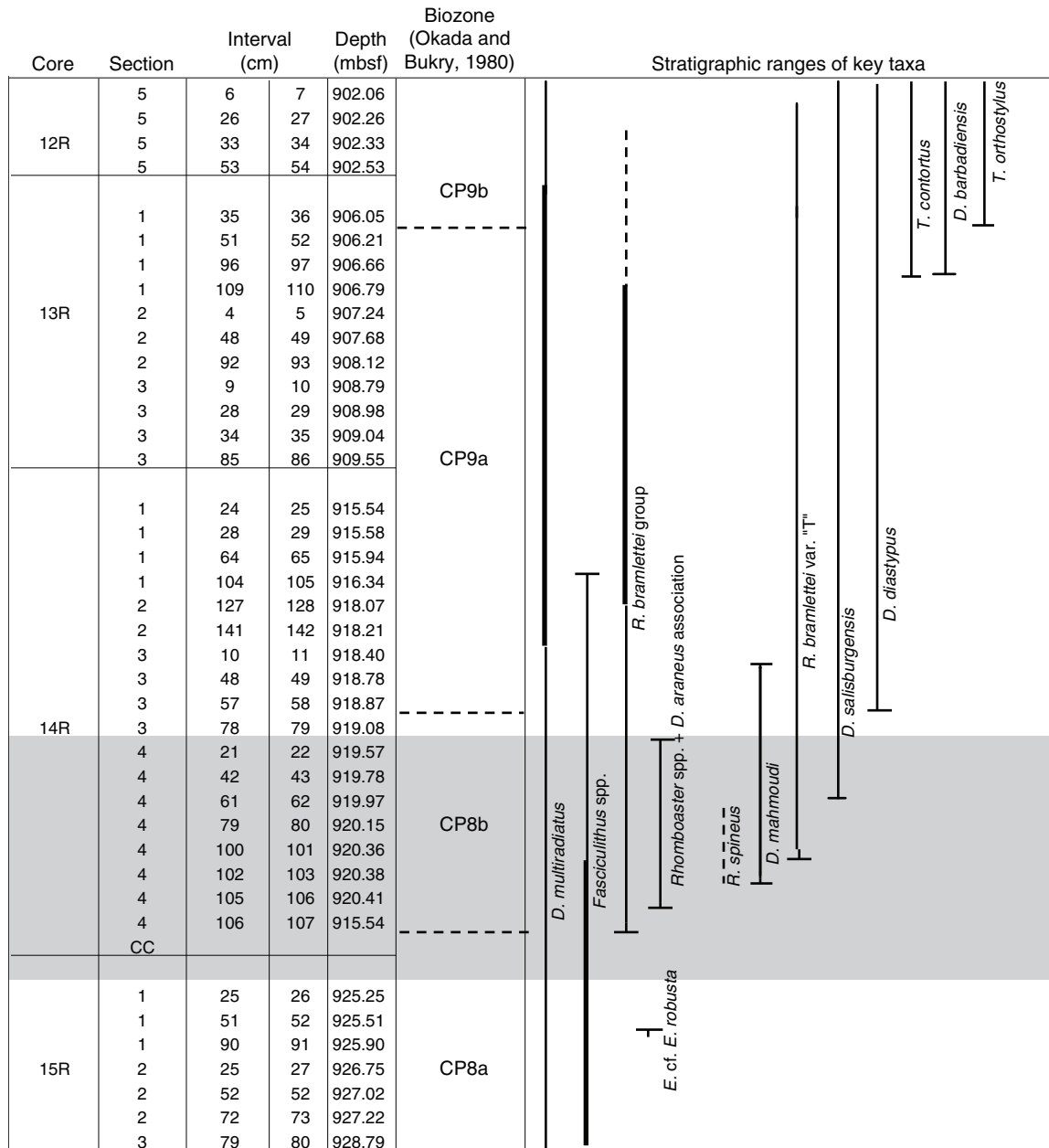


Figure F7. Age-depth plot for Site 1276. Oligo. = Oligocene; Paleoc. = Paleocene; Ma. = Maastrichtian; Campan. = Campanian; S. = Santonian; C. = Coniacian; T. = Turonian; Cen. = Cenomanian; A. = Aptian. Average sedimentation rate segments (m/m.y.) are discussed in text; also see Table T1, p. 48.

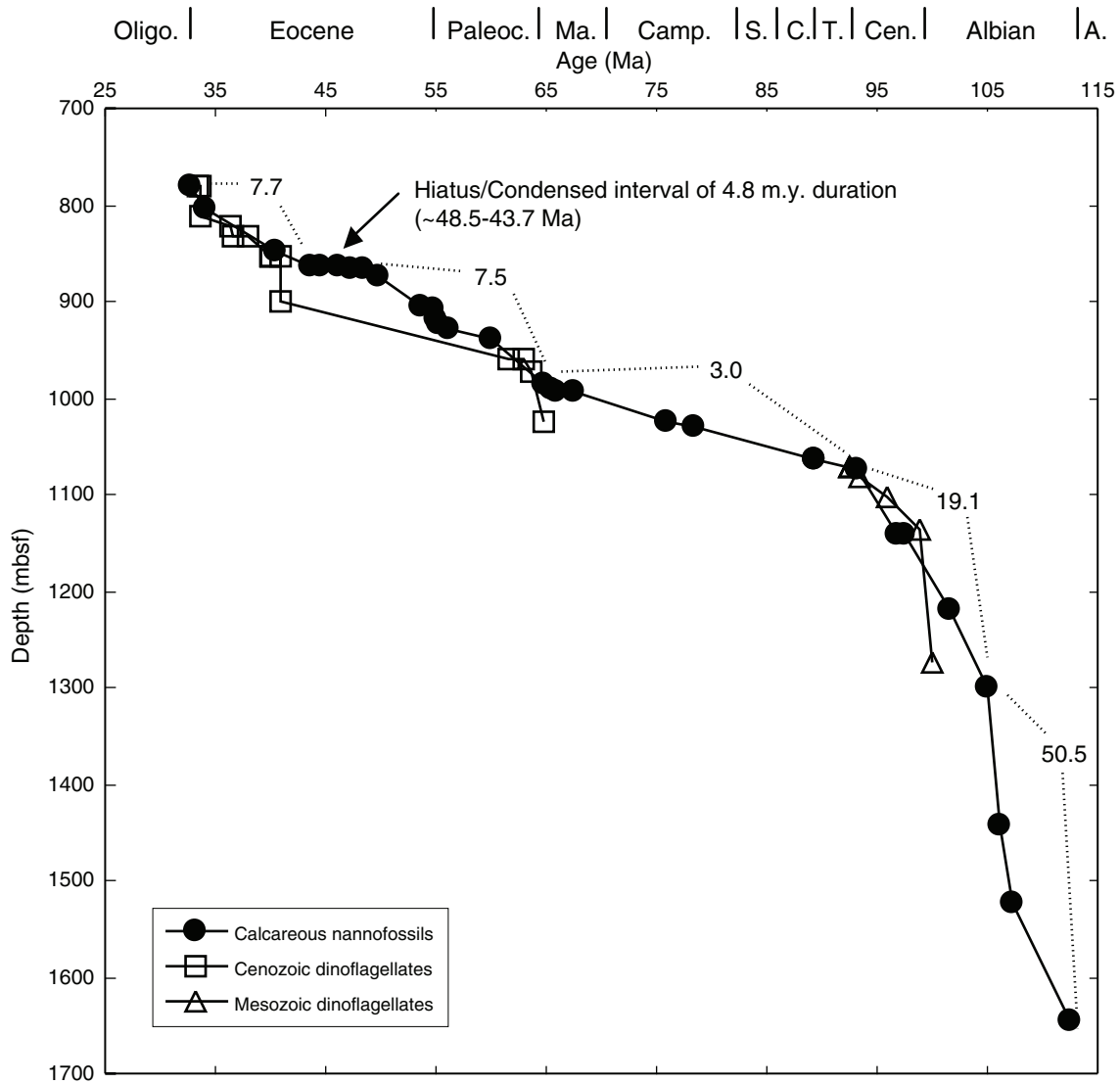


Table T1. Biostratigraphic datums used in age-depth plot for Site 1276 (see Fig. F7, p. 47).

Age-depth datum	Age (Ma)	Occurrence		Nonoccurrence		Median depth
		Depth (mbsf)	Core, section, interval (cm)	Depth (mbsf)	Core, section, interval (cm)	
		210-1276A-		210-1276A-		
Cenozoic nannofossil						
FO <i>Chiasmolithus altus</i>	32.8	759.19	1W-CC	801.44	2R-1, 144-145	780.32
LO <i>Markalius inversus</i> /FO <i>C. subdistictus</i>	34.2	803.51	2R-CC	803.36	2R-3, 36-37	803.44
LO <i>Chiasmolithus solitus</i>	40.4	848.43	7R-1, 43-44	848.26	7R-1, 26-27	848.35
FO <i>Reticulofenestra umbilica</i>	43.7	863.80	8R-5, 20-21	863.84	8R-5, 24-25	863.82
LO <i>C. gigas</i>	44.5	864.91	8R-5, 131-132	864.86	8R-5, 126-127	864.89
FO <i>C. gigas</i>	46.1	864.91	8R-5, 131-132	864.96	8R-5, 136-137	864.94
LO <i>Rhabdosphaera inflata</i>	47.3	865.11	8R-6, 1-2	865.06	8R-5, 146-147	865.09
FO <i>Rhabdosphaera inflata</i>	48.5	866.13	8R-CC	867.49	9R-1, 29-31	866.81
FO <i>Discoaster subloboensis</i>	49.7	873.72	9R-5, 52-53	874.48	9R-5, 128-129	874.10
FO <i>Tribrachiatius orthostylus</i>	53.6	906.05	13R-1, 35-36	906.21	13R-1, 51-52	906.13
FO <i>Tribrachiatius contortus</i>	54.7	906.66	13R-1, 109-110	906.79	13R-1, 109-110	906.73
FO <i>Discoaster diastypus</i>	55.0	918.87	14R-3, 57-58	919.08	14R-3, 78-79	918.98
LO <i>Fasciculithus tympaniformis</i>	55.3	928.77	14R-1, 104-105	915.94	14R-1, 64-65	922.36
FO <i>Discoaster multiradiatus</i>	56.2	928.77	15R-3, 77-78	929.76	15R-4, 26-27	929.27
FO <i>Fasciculithus ulii</i>	59.9	938.22	16R-3, 72-73	939.61	16R-4, 65-66	938.92
FO <i>Cruciplacolithus primus</i>	64.8	986.59	21R-3, 113-114	986.79	21R-3, 133-134	986.69
Mesozoic nannofossil						
FO <i>Micula prinsii</i>	65.4	988.32	21R-CC	992.42	22R-1, 2-3	990.37
FO <i>Nephrolithus frequens</i>	65.8	992.48	22R-1, 8	994.39	22R-2, 50-51	993.44
FO <i>Lithraphidites quadratus</i>	67.5	992.48	22R-1, 8	994.39	22R-2, 50-51	993.44
FO <i>Uniplanarius trifidus</i>	76.0	1023.79	25R-2, 109-110	1024.40	25R-3, 20-21	1024.10
FO <i>Ceratolithoides aculeus</i>	78.5	1027.68	25R-5, 48-49	1031.21	26R-1, 41-42	1029.45
FO <i>Lithastrinus septenarius</i>	89.3	1061.36	29R-2, 22-23	1065.74	29R-5, 21-22	1063.55
FO <i>Marthasterites furcatus</i>	89.3	1061.36	29R-2, 22-23	1065.74	29R-5, 21-22	1063.55
FO <i>Quadrum gartneri</i>	93.2	1072.71	30R-3, 58-59	1075.31	30R-5, 18-19	1074.01
FO <i>Lithraphidites acutus</i>	96.8	1141.83	37R-5, 18-19	1143.38	37R-6, 32-33	1142.61
FO <i>Corollithion kennedyi</i>	97.6	1141.83	37R-5, 18-19	1143.38	37R-6, 32-33	1142.61
FO <i>Eiffellithus turriseiffellii</i>	101.7	1220.06	45R-3, 130-131	1217.52	45R-4, 13-14	1218.79
FO <i>Eiffellithus monechiae</i>	105.0	1300.47	53R-6, 46-47	1301.02	54R-1, 142-143	1300.75
FO <i>Axopodorhabdus albianus</i>	106.1	1442.48	69R-2, 118-119	1443.60	69R-3, 80-81	1443.04
FO <i>Tranolithus orionatus</i>	107.3	1521.65	77R-3, 51-52	1522.51	77R-4, 111-112	1522.08
FO <i>Hayesites albiensis</i>	112.5	1678.94	94R-5, 136-137	1679.82	94R-6, 73-74	1646.10
Cenozoic dinoflagellate cyst						
LO <i>Lentinia serrata</i>	33.5	803.51	2R-CC	759.19	1R-CC	781.35
FO <i>Areoligera semicirculata</i>	33.7	759.19	1W-CC	803.51	2R-CC	781.35
LO <i>Hemiplacophora semilunifera</i>	33.6	819.26	3R-CC	803.51	2R-CC	811.39
FO <i>Hemiplacophora semilunifera</i>	36.4	819.26	3R-CC	825.90	4R-CC	822.58
FO <i>Enneadocysta pectiniformis</i>	36.5	825.90	4R-CC	838.15	5R-CC	832.03
LO <i>Cerebrocysta bartonensis</i>	38.0	838.15	5R-CC	825.90	4R-CC	832.03
FO <i>Lentinia serrata</i>	40.0	847.40	6R-CC	857.68	7R-CC	852.54
FO <i>Rhombodinium draco</i>	40.0	847.40	6R-CC	857.68	7R-CC	852.54
FO <i>Cordosphaeridium cantharellum</i>	40.8	847.40	6R-CC	857.68	7R-CC	852.54
FO <i>Cerebrocysta bartonensis</i>	41.0	857.68	7R-CC	942.23	16R-CC	899.96
FO <i>Alisocysta margarita</i>	61.7	953.66	17R-CC	963.40	18R-CC	958.53
LO <i>Oligosphaeridium pulcherrimum</i>	63.0	963.40	18R-CC	953.66	17R-CC	958.53
LO <i>Spongodinium delitiense</i>	63.7	982.82	20R-CC	963.40	18R-CC	973.11
FO <i>Damassadinium californicum</i>	64.8	982.82	20R-CC	1067.61	29R-CC	1025.22
Mesozoic dinoflagellate cyst						
LO <i>Litosphaeridium siphoniphorum</i>	92.4	1076.64	30R-CC	1067.61	29R-CC	1072.13
FO <i>Senoniasphaera rotundata alveolata</i>	92.5	1067.61	29R-CC	1076.64	30R-CC	1072.13
FO <i>Chatangiella verrucosa</i>	93.5	1076.64	30R-CC	1086.88	31R-CC	1081.76
LO <i>Ovoidinium verrucosum</i>	95.8	1107.76	33R-CC	1098.33	32R-CC	1103.05
FO <i>Xiphophoridium alatum</i>	98.9	1164.03	39R-CC	1107.76	33R-CC	1135.90
FO <i>Palaeohysterochophora infusorioides</i>	99.9	1221.50	45R-CC	1324.66	56R-CC	1273.08

Note: FO = first occurrence, LO = last occurrence.

Plate P1. Albian. All micrographs are cross-polarized light images. **1.** *Lithraphidites alatus* (Sample 210-1276A-86R-3, 77 cm). **2, 3.** *Helicolithus trabeculatus* (Sample 210-1276A-94R-6, 73 cm); (3) rotated. **4.** *Broinsonia* cf. *Broinsonia viriosa* (Sample 210-1276A-96R-5, 92 cm). **5.** *Hayesites irregularis* (Sample 210-1276A-96R-2, 76 cm). **6, 7.** *Hayesites albiensis*; (6) Sample 210-1276A-67R-3, 12 cm; (7) Sample 210-1276A-94R-5, 136 cm. **8.** *Eiffellithus hancockii* (Sample 210-1276A-94R-6, 73 cm). **9.** *Prediscosphaera spinosa* (Sample 210-1276A-94R-6, 74 cm). **10–12.** *Prediscosphaera columnata*; (10) subcircular (Sample 210-1276A-95R-5, 116 cm); (11) circular (Sample 210-1276A-95R-3, 112 cm); (12) circular (Sample 210-1276A-95R-1, 103 cm). **13.** *Seribiscutum primitivum* (Sample 210-1276A-85R-4, 111 cm). **14.** *Prediscosphaera columnata* side view (Sample 210-1276A-80R-5, 63 cm). **15, 16.** Sample 210-1276A-37R-5, 18 cm; (15) *Tranolithus praeorionatus*; (16) *Tranolithus orionatus*.

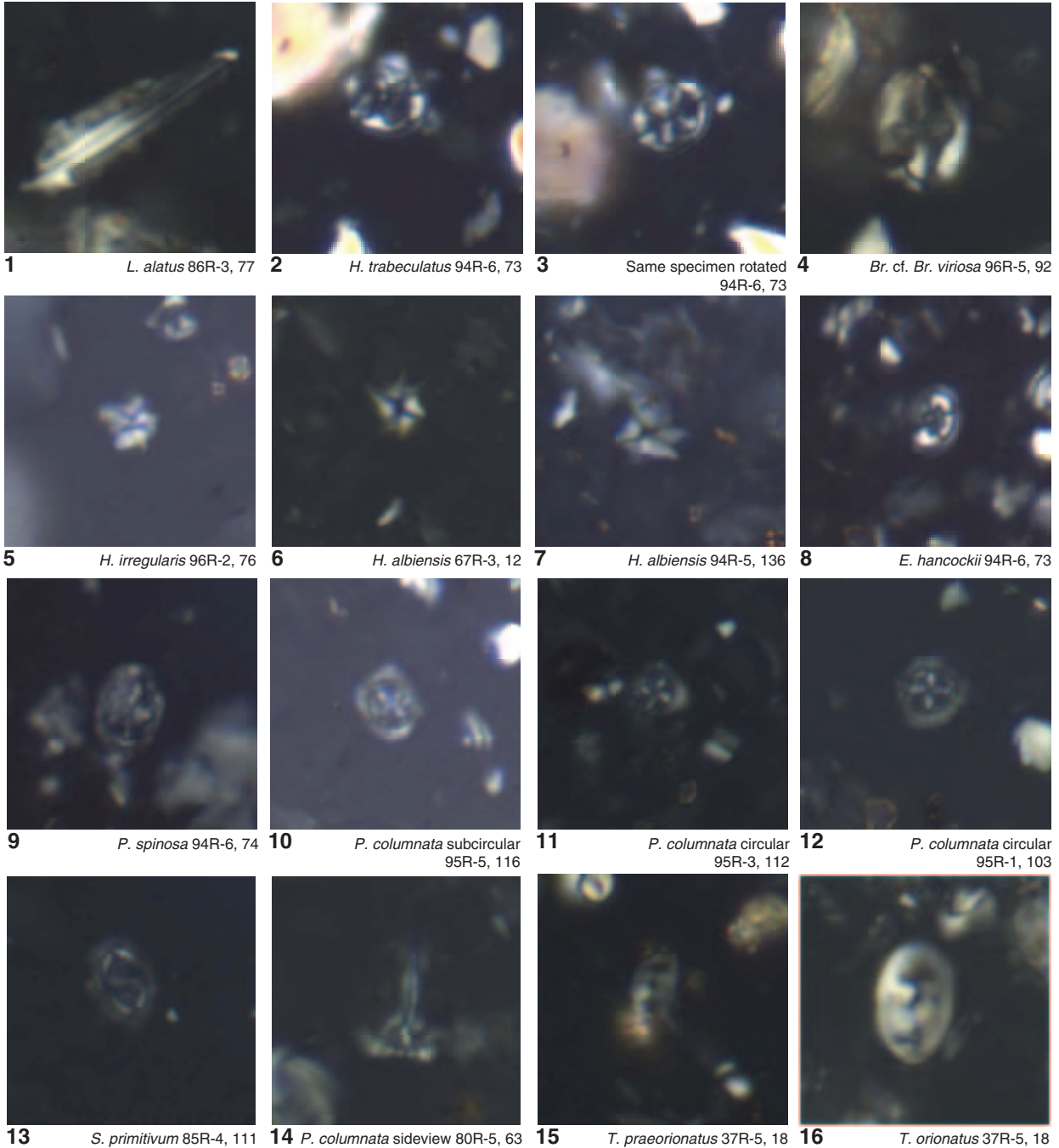


Plate P2. Cenomanian–Turonian. Micrographs with dark background are cross-polarized light images; those with light background are natural-light images. 1. *Lithraphidites acutus* (Sample 210-1276A-37R-4, 38 cm). 2. *Gartnerago nanum* (Sample 210-1276A-36R-4, 14 cm). 3. *Lucianorhabdus maleformis* (Sample 210-1276A-29R-2, 22 cm). 4. *Corollithion kennedyi* (Sample 210-1276A-36R-CC). 5. *Quadrum gartneri* (Sample 210-1276A-29R-5, 21 cm). 6. *Acaenolithus cenomanicus* (Sample 210-1276A-35R-3, 58 cm). 7, 11, 13. (Sample 210-1276A-29R-2, 22 cm); (7) *Eiffellithus eximius* (11) *Marthasterites furcatus*; (13) *Eprolithus eptapetalus*. 8. *Lithastrinus septenarius* (Sample 210-1276A-29R-1, 18 cm). 9. *Axopodorhabdus albianus* (Sample 210-1276A-69R-2, 118 cm). 10. *Ahmuellerella octoradiata* (Sample 210-1276A-30R-3, 54 cm). 12. *Eprolithus octopetalus* (Sample 210-1276A-30R-1, 49 cm). 14. *Gartnerago theta* (210-1276A-34R-1, 4 cm). 15, 16. *Cretarhabdus loriei* (Sample 210-1276A-32R-7, 66 cm); (16) same specimen rotated. 17. *Rhagodiscus asper* (Sample 210-1276A-34R-2, 127 cm).

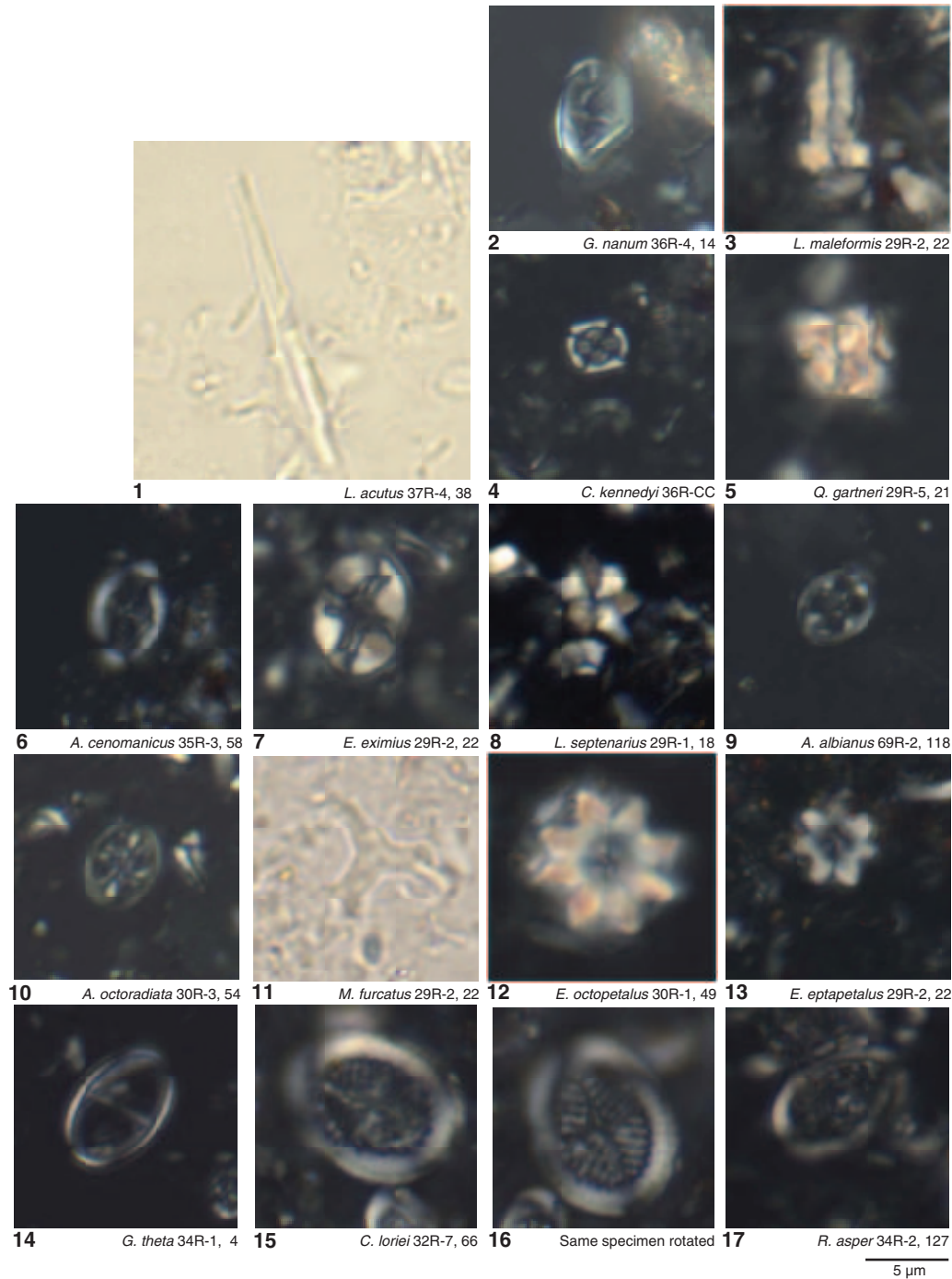
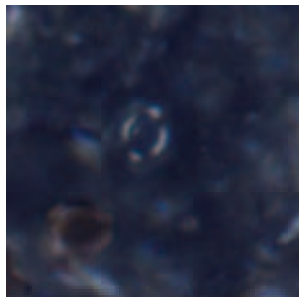
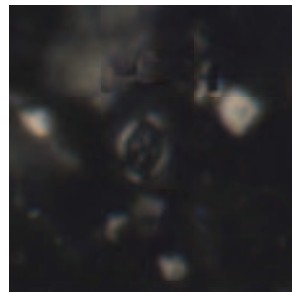
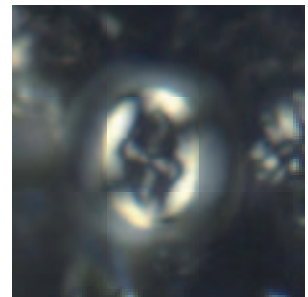
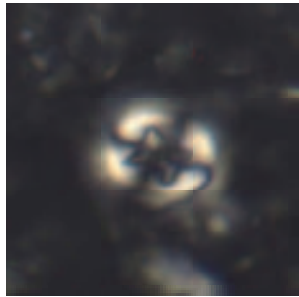
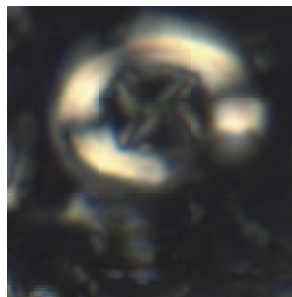
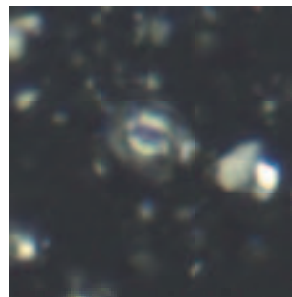
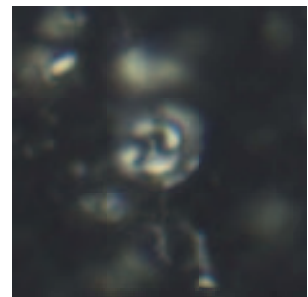
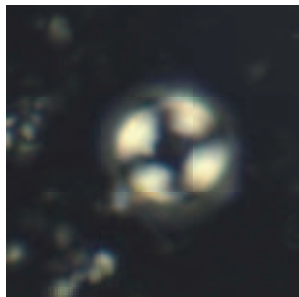
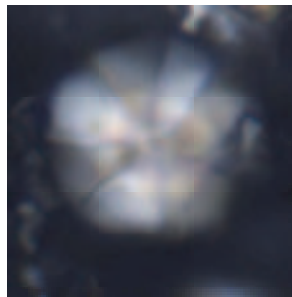
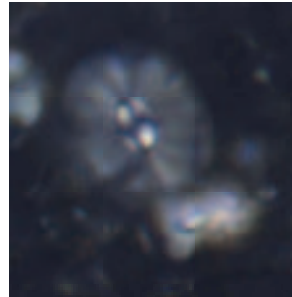
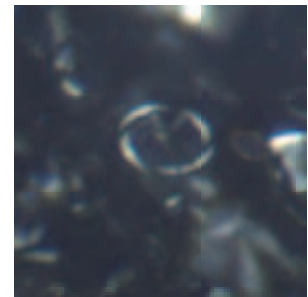
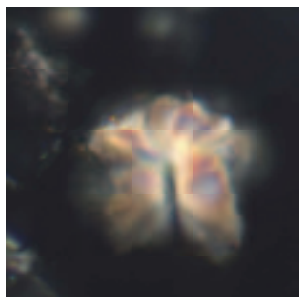
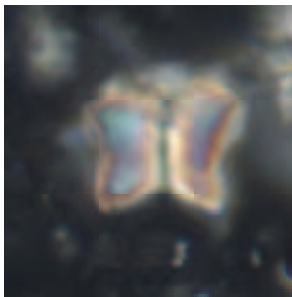
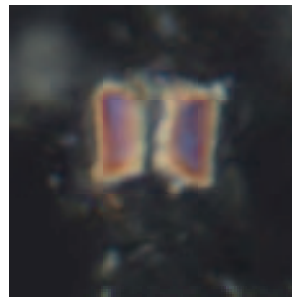
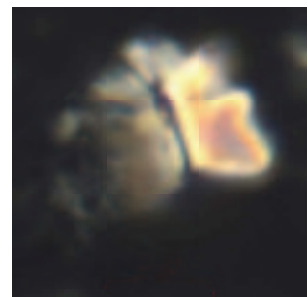
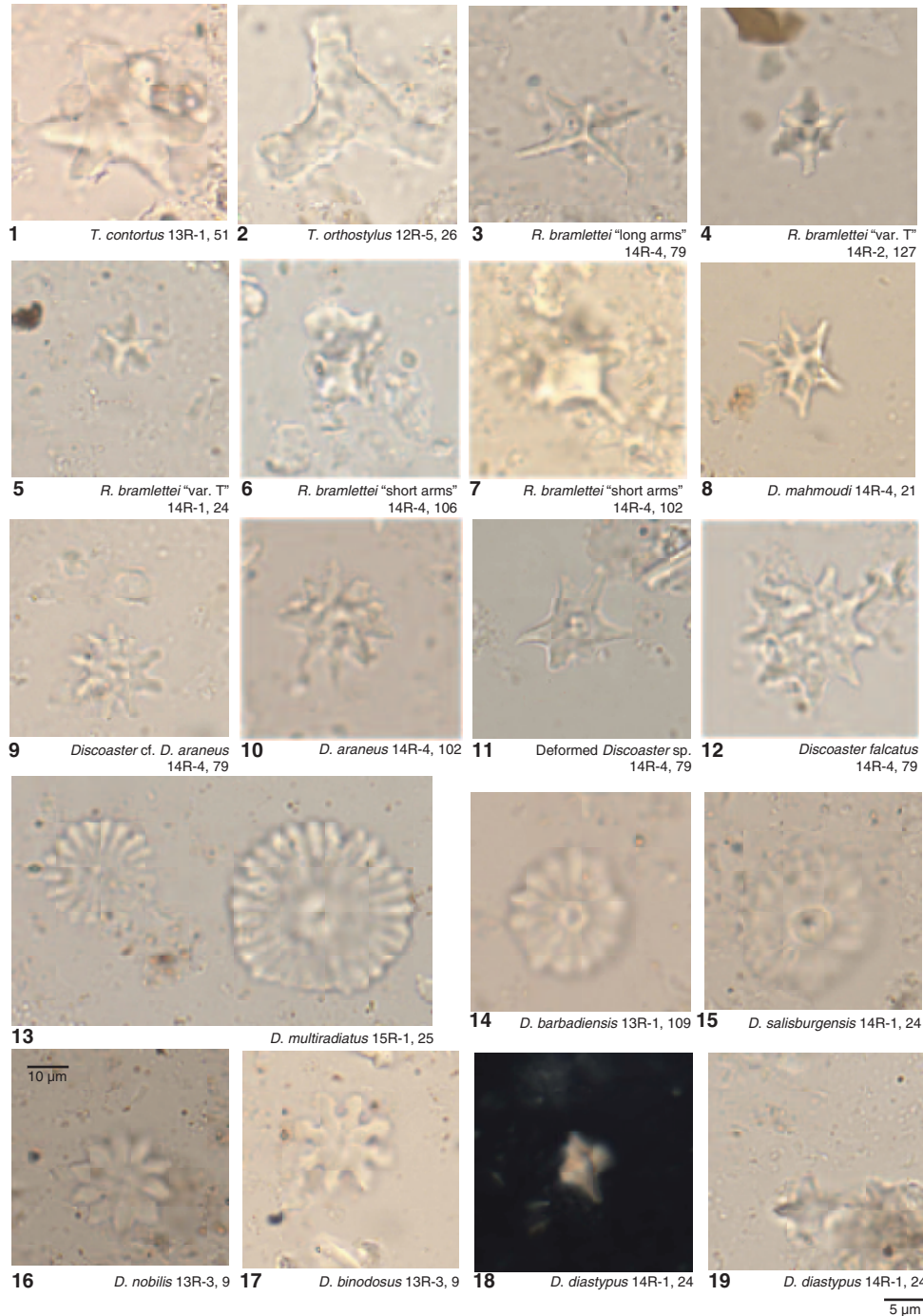


Plate P3. Danian. All micrographs are cross-polarized light images. 1, 4, 12. Sample 210-1276A-20R-4, 149 cm; (1) *Crucioplacolithus primus*; (4) *Crucioplacolithus asymmetricus*; (12) *Neochiastozygus concinnus*. 2, 3, 10, 11. Sample 210-1276A-20R-5, 97 cm; (2) *Crucioplacolithus primus*; (3) *Crucioplacolithus intermedius*; (10) *Bianolithus sparsus*; (11) *Markalius panis*. 5, 9. Sample 210-1276A-19R-4, 96 cm; (5) *Ch. danicus*; (9) *Ericsonia subpertusa*. 6. *Chiasmolithus bidens* (Sample 210-1276A-15R-2, 26 cm). 7, 8. Sample 210-1276A-18R-7, 45 cm; (7) *Toweius* cf. *T. pertusus*; (8) *Prinsius bisulcus*. 13, 16. Sample 210-1276A-15R-2, 25 cm; (13) *Fasciculithus* sp.; (16) *Fasciculithus tonii*. 14, 15. Sample 210-1276A-16R-3, 72 cm; (14) *Fasciculithus* cf. *ulii*; (15) *Fasciculithus involutus*.

1 *Cr. primus* 20R-4, 1492 *Cr. primus* 20R-5, 973 *Cr. intermedius* 20R-5, 974 *Cr. asymmetricus* 20R-4, 1495 *Ch. danicus* 19R-4, 966 *Ch. bidens* 15R-2, 267 *Toweius* cf. *T. pertusus*
18R-7, 458 *P. bisulcus* 18R-7, 459 *E. subpertusa* 19R-4, 9610 *B. sparsus* 20R-5, 9711 *M. panis* 20R-5, 9712 *Ne. concinnus* 20R-4, 14913 *Fasciculithus* sp. 15R-2, 2514 *F. cf. F. ulii* 16R-3, 7215 *F. involutus* 16R-3, 7216 *F. tonii* 15R-2, 25

5 μm

Plate P4. Paleocene–Eocene. All micrographs are natural-light images except image 18, which is a cross-polarized light image. 1. *Tribrachiatus contortus* (Sample 210-1276A-13R-1, 51 cm). 2. *Tribrachiatus orthostylus* (Sample 210-1276A-12R-5, 26 cm). 3, 9, 11, 12. (Sample 210-1276A-14R-4, 79 cm; (3) *Rhomboaster bramlettei* “long arms;” (9) *Discoaster* cf. *D. araneus*; (11) deformed *Discoaster* sp.; (12) *Discoaster falcatus*. 4. *Rhomboaster bramlettei* “var. T” (Sample 210-1276A-14R-2, 127 cm). 5, 15, 18, 19. Sample 210-1276A-14R-1, 24 cm; (5) *Rhomboaster bramlettei* “var. T;” (15) *Discoaster salisburgensis*; (18, 19) *Discoaster diastypus*. 6. *Rhomboaster bramlettei* “short arms” (Sample 210-1276A-14R-4, 106 cm). 7, 10. Sample 210-1276A-14R-4, 102 cm; (7) *Rhomboaster bramlettei* “short arms;” (10) *Discoaster araneus*. 8. *Discoaster mahmoudii* (Sample 210-1276A-14R-4, 21 cm). 13. *Discoaster multiradiatus* (Sample 210-1276A-15R-1, 25 cm). 14. *Discoaster barbadiensis* (Sample 210-1276A-13R-1, 109 cm). 16, 17. Sample 210-1276A-13R-3, 9 cm; (16) *Discoaster nobilis*; (17) *Discoaster binodosus*.



CHAPTER NOTES*

- N1. Wood, A.S., Gardin, S., and Wise, S.W., Jr., submitted. Age constraint and interpretations of a disconformity in the Newfoundland-Iberia rift basin, ODP Leg 210. *Rev. Micropaleontol.*
- N2. Georgescu, M.D., Leckie, R.M., and Hiscott, R.N., submitted. Latest Paleocene and early Eocene large-sized reworked benthic foraminifers in the Newfoundland Basin (ODP Leg 210, Site 1276) and their paleoclimatic significance. *Rev. Micropaleontol.*

*Dates reflect file corrections or revisions.